CHEMICAL REVIEWS

Review

pubs.acs.org/CR

Actinide Colloids and Particles of Environmental Concern

Clemens Walther*,† and Melissa A. Denecke‡

†Institute for Radioecology and Radiation Protection, Leibniz University Hannover, Herrenhäuser Strasse 2, D-30419 Hannover, Germany

‡Institute for Nuclear Waste Disposal, Karlsruhe Institute of Technology, P.O. Box 3640, D-76021 Karlsruhe, Germany

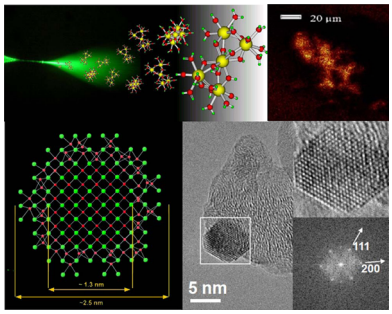

Downloaded via LOS ALAMOS NATL LABORATORY on June 10, 2025 at 17:41:54 (UTC).
See https://pubs.acs.org/sharingguidelines for options on how to legitimately share published articles.

CONTENTS

1. Introduction 995
2. Environmental Actinide Particles 996
  2.1. Particles from Naturally Occurring Radioactive Matter 996
  2.2. "Hot" Particles Released in the Environment 998
    2.2.1. "Hot" Actinide Particles from Military Nuclear Devices 999
    2.2.2. Nanoparticles from Depleted Uranium (DU) 999
    2.2.3. "Hot" Actinide Particles from Reprocessing of Nuclear Material and Accidents 1000
    2.2.4. Colloid-Mediated Transport 1002
3. Aerosols/Safeguards 1003
4. Synthetic Particles 1005
  4.1. Reference Actinide Particles 1005
  4.2. Actinide Nanoparticles in Solution 1005
    4.2.1. Detection of Actinide Particles in Solution 1005
    4.2.2. Thorium Colloids 1006
    4.2.3. Neptunium and Uranium Colloids 1006
    4.2.4. Plutonium Nanoparticles 1007
  4.3. Well-Defined Nanoparticles and Clusters 1008
5. Conclusion and Outlook 1010
Author Information 1010
  Corresponding Author 1010
  Notes 1010
  Biography 1011
References 1011

1. INTRODUCTION

The radioecological relevance of actinide particles[1] did not first become a matter of concern following the nuclear accidents at Fukushima, Chernobyl, or Three Mile Island. Public and scientific attention was directed to the potential hazards of actinide particles soon after the first production and use of actinide elements in the 1940s. Above ground atomic explosions caused tremendous amounts of radioactive fallout with a considerable fraction present as particles, which were easily dispersed over wide distances.[2] As early as the 1950s and 1960s, several studies appeared dealing with the aerosol transport mechanisms of radionuclides in general[3] and actinides in particular.[4]

Sources of actinide particles in the environment other than nuclear explosions and nuclear power plant accidents are naturally occurring radioactive matter or particle contaminants released from other military activities (e.g., nuclear submarines, ammunition), from activities related to nuclear power production (e.g., mining and fuel fabrication), and also from minor occurrences such as nuclear powered satellites.[5] Such particles (nanometer- or submicrometer- to micrometer-sized particles) containing actinide element contaminants (actinide containing particles) are found in the environment in a wide variety of forms or morphologies and compositions, exhibiting varying chemistries and stabilities, for example, as pure actinide or actinide oxide particles (referred to as intrinsic actinide particles), as single element or mixed oxides, and as solid solutions in various phases, to name a few.

Radioactive contaminant particles are often referred to as "hot" particles (and not necessarily limited to actinide containing particles), although this definition is qualitative and does not signify a defined level of radioactivity. The analysis of the isotope content of environmental actinide containing particles gives information concerning its origin. This information can also be used for safeguards against proliferation. Characterization of the speciation or chemical and physical state of actinides in nano- or micrometer-sized particles can shed light on their potential to dissolve, to be transported in the environment (geo-, hydro-spheres), and to ultimately be transferred to the ecosystem (biosphere), which is essential for predicting safety of nuclear waste repositories, evaluating the effectiveness of remediation strategies, and assessing bioavailability and related potential to exert negative health effects. Heterogeneous actinide containing particles comprised of multiple phases, as well as different elements and isotopes, present a challenge for their analysis, characterization, and prediction of their behavior. Modern instrumentation developments and studies of laboratory and reference systems are helping researchers meet this challenge.

The morphology and elemental and isotopic composition of actinide (containing) particles can be obtained by a great variety of experimental techniques,[5,6] such as electron

Special Issue: 2013 Nuclear Chemistry

Received: August 16, 2012
Published: January 15, 2013

 © 2013 American Chemical Society dx.doi.org/10.1021/cr300343c | Chem. Rev. 2013, 113, 995–1015

microscopy[7] (including transmission EM, TEM;[8] scanning EM, SEM; EM with secondary X-ray spectroscopy, Auger spectroscopy, electron energy loss spectroscopy EELS, etc.), mass spectrometry[9] (including inductively coupled plasma MS, ICP MS;[10] accelerator MS, AMS;[11] secondary ion MS, SIMS;[12] electrospray MS, ESI-MS[13]), matrix assisted laser desorption MS, MALDI-MS;[14] resonant ionization MS, RIMS;[15] thermal ionization MS, TIMS), X-ray-based methods[16] (including scattering, absorption, emission, (spectro)microscopy), and many more. Application of such state-of-the-art techniques to characterize nanometer- to micrometer-sized particles in the solid state and in solution (colloids and multinuclear species), which contain actinide elements and, hence, of environmental concern is presented below. For a review of the techniques themselves, the reader is referred to refs 5,6.

In this Review, a cross-section of the present knowledge concerning actinide containing particles of both environmental as well as synthetic origin is presented. The synthetic systems serve as reference material and models for understanding the formation, reactivity, and structure of environmental actinide containing particles. The reader is also referred to the first book published covering different aspects of research on actinide nanoparticles.[17] This Review is structured according to the actinide particles' origin. Section 2.1 focuses on particles present in natural radioactive matter and in technically enhanced radioactive matter. Section 2.2 deals with actinide containing particles present in the environment due to anthropogenic activities and includes discussion of particle speciation and its effect on weathering and mobility. The importance of colloid-mediated transport in the migration of radioactivity in the environment is reflected in our including a dedicated section for this topic (section 2.2.4). Aerosols and "hot" particles and their use in nuclear safeguards are discussed in section 3. Synthetic actinide particles as reference material (section 4.1) and model systems are the topic of section 4. Section 4.2 covers actinide particles in solution (colloids), and included in sections 4.2.2−4.2.4 is material on synthetic thorium, uranium, neptunium, plutonium particles, and colloidal species in solution with an emphasis on plutonium. Selected recent results on well-defined actinide nanoparticles and clusters (section 4.3) are presented at the close of section 4. At the end of this treatise, we conclude by highlighting the need for further research in this area, especially in light of potential effects of such particles on human health and the worldwide growing need for energy, and briefly outline our outlook for future activities in this area of research (section 5).

2. ENVIRONMENTAL ACTINIDE PARTICLES

2.1. Particles from Naturally Occurring Radioactive Matter

Radioactive particles are not necessarily of anthropogenic origin; rather they can be present as naturally occurring radioactive matter (NORM). For example, small grains of Th-bearing and U-bearing minerals, which occur naturally in soil and sediments, are considered radioactive particles.[6,18] The morphology, structure, composition, and size of such particles evolve from the intricate interplay of numerous parameters, including paragenesis, redox conditions, and temperature, to name a few. Deditius and co-workers[19] reported from transmission electron microscopy (TEM) investigations (high-resolution TEM, HRTEM; high angle annular dark field scanning transmission electron microscopy, HAADF-STEM; energy dispersive X-ray spectroscopy, TEM-EDX) formation of nanocrystalline thorium bearing coffinite ((U,Th)-$SiO_4{\cdot}nH_2O$, n = 0−2), measuring 20−40 nm in size (see Figure 1) with characteristic Th/U ratios of 0.6, associated with

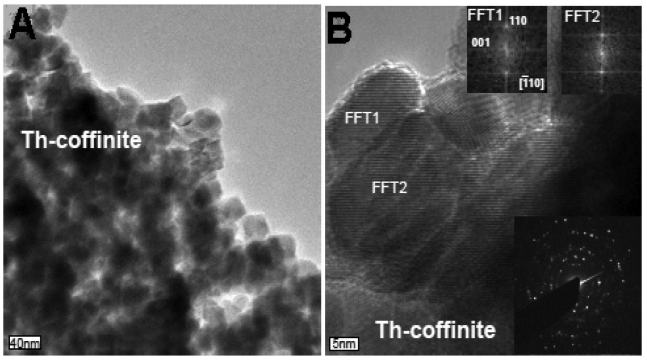

Figure 1. (A) HRTEM image of nanoparticles of Th-coffinite formed on U bearing thorite. (B) Higher resolution image with SAED at lower right and two FFT, indicating misalignment and similar alignment of crystals, respectively. Reproduced with permission from ref 19. Copyright 2012 Mineralogical Society of America.

amorphous uranium bearing thorite ($(Th,U)SiO_4{\cdot}nH_2O$), having measured Th/U ratios 10 times higher. The same group observed coffinite formation as crystallites as large as 100 nm at edges of altered carbonate fluorapatite ($Ca_5(PO_4,CO_3)_3F$) crystals under Si-rich reducing conditions, but formation of metaautunite ($M[(UO_2)(PO_4)]2(H_2O)_6$, M = alkaline earth) at the expense of coffinite and fluorapatite occurred under P-rich oxidizing conditions.[20] Uranium and rare-earth elements incorporated into nanoscale crystals of secondary coffinite have also been reported.[21]

Finch and Murakami[22] gave an extensive review on uranium ore chemistry, including a special focus on alteration and how Pb exogenesis alters uranium minerals. Uranyl phosphate paragenesis, for instance, leads to formation of submicrometer-sized crystallites even under global U/P concentrations well below saturation for the solid phase due to microcrystallization processes under local saturation conditions.[23]

Incorporation of α-emitting thorium and uranium isotopes into mineral crystallites leads to metamictization or formation of amorphous domains due to radiation damage. This has been extensively studied for zircon, $ZrSiO_4$.[24−26] The amorphatized or glass metamict phase has a higher dissolution rate, which leads to a higher chemical mobility of the actinides from weathering of zircon particles in soil with high levels of radiation damage.[27]

Little has been published on technically enhanced NORM (TENORM) actinide particles. TENORM particles stem from natural occurring material that has been released through various human activities, including mining, energy production, and waste. Nuclear emulsion microscopy was employed to demonstrate the presence of small, intense α-particle emitting crystallites in tailings derived from the sulfuric acid milling of uranium ores.[18] Thorium, U, and daughter nuclides such as $^{210}Po/^{210}Pb$ may be heterogeneously distributed in minerals, thus occurring as hot spots in U mining and tailing samples. Recently, single grains of U minerals have been isolated from soil samples originating from former U mining sites in Kazakhstan and Kyrgyzstan[6] and references therein. Heterogeneities (i.e., U hot spots) have also been observed on surfaces of Norwegian mineral specimens[6(and references therein)] by environ-

dx.doi.org/10.1021/cr300343c | Chem. Rev. 2013, 113, 995−1015

mental scanning electron microscopy (SEM). Another TENORM example was reported by Utsunomiya and Ewing using HRTEM.[28] In their study of atmospheric emissions from coal fired power plants, they characterized actinide containing particles found in the fine fraction. Typically, Th originates from soil-derived particles, whereas U, concentrated in the finest fractions, originates from combustion of fossil fuels. Surprisingly, the UO_{2+x} particles associated with particulate emissions were found coated by a fullerene cage, hence making them more inert to environmental erosion and leaching (see Figure 2, from ref 29).

Another formation mechanism of actinide NORM nanoparticles occurring in nature is biomineralization/bioprecipitation of dissolved forms of uranium.[30,31] Such microbial-mediated formed minerals are typically nanometer-sized and in hydrous phases, rendering them difficult to characterize in situ. Fayek et al.[32] combined nanoscale secondary-ion mass spectrometry (nanoSIMS) and advanced HRTEM to characterize the surfaces of *Geobacter sulfurreducens* and associated bioprecipitated uranium phases (prepared in the laboratory as model systems). Uranium was observed to be precipitated on the bacteria surface as nanocrystals of uraninite (UO_2). In other studies, extracellular and periplasmic uranium nanoparticle formation has been reported (see ref 33 and references therein).

Microbes other than Fe(III) reducing bacteria such as members of the *Geobacter* and *Shewanella* species are also capable of reducing U(VI) to less-soluble U(IV) such as *Clostridium* species and *Desulfovibrio* sulfate-reducing bacteria (see ref 34 and references therein). The mechanism of reduction is via direct enzymatic pathways or indirectly via biogenerated Fe(II). Biosequestration of uranium is often enhanced by addition of (electron donor) nutrients such as acetic acid and fatty acids.[35] The results in ref 32 suggest that biofilms formed over the biogenic nanoparticles, which shielded the UO_2 from reoxidation to the more mobile U(VI). Hence, biotransformations under certain conditions can immobilize uranium for extended periods, even under relatively oxidizing conditions in the subsurface.

Bargar and co-workers[36] have studied the structure and dissolution of biogenic UO_2. Synchrotron-based methods (X-ray diffraction, XRD and extended X-ray absorption fine structure, EXAFS) show that the biogenic ~2.5 nm particles used in dissolution investigations were structurally ordered (Figure 3) with the cubic UO_2 structure.[37] Its dissolution in laboratory studies of aqueous solutions containing dissolved inorganic carbon (DIC as $NaHCO_3$), however, was significantly greater.[38] Enhanced dissolution in the presence of carbonate in near neutral conditions suggests that detachment of surface species other than U(IV) (forms weak carbonate complexes) was involved. Identification of surface U(V) and U(VI) species on nanoparticle UO_2 surfaces from X-ray photoelectron spectroscopy (XPS) results[39] indicates that the nanoparticle surface is continuously oxidized (even in reducing conditions). Penta- and hexavalent uranyl cations form carbonate complexes ($[UO_2(CO_3)_x]^{2x-1}$, $[UO_2(CO_3)_x]^{2x-2}$) in neutral solutions so that dissolution in anoxic conditions in the presence of DIC may be controlled by carbonate complexation of these species on the surface and subsequent detachment. The underlying reason for the higher dissolution rate of biogenic UO_2 in aqueous solutions containing DIC is the high amount of U(V)/U(VI) on its surface.

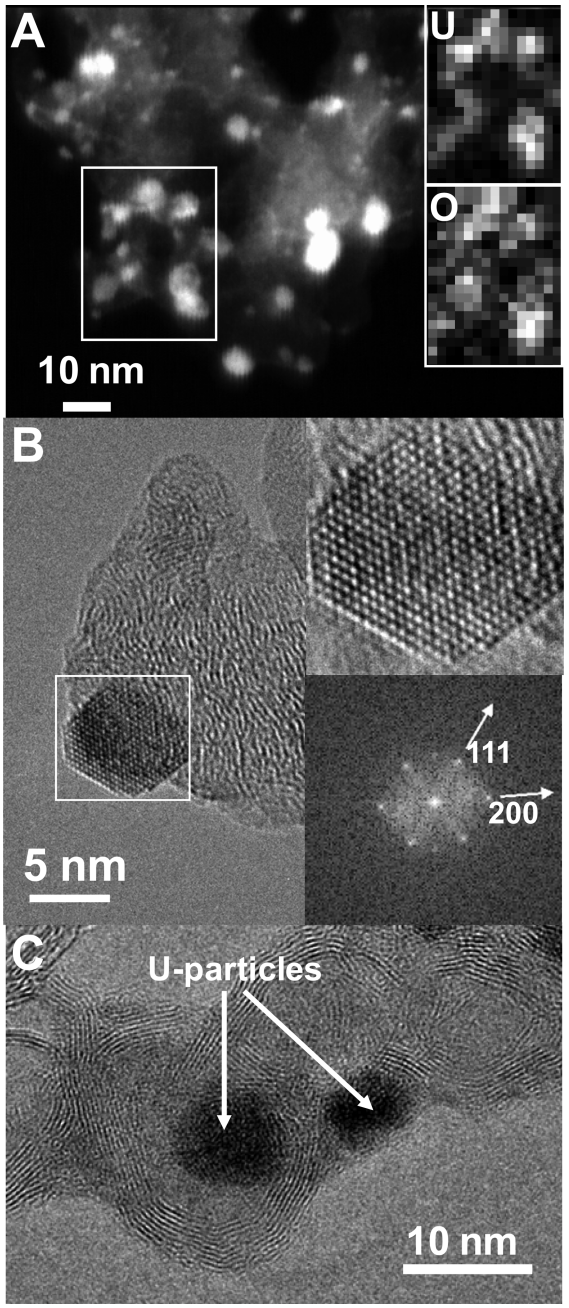

Figure 2. Application of HAADF-STEM to characterize uraninite nanoparticles in the atmospheric particulates:[13] (a) HAADF-STEM image of the area reveals the occurrence of many heavy particles less than 10 nm in size. The insets are elemental maps of uranium and oxygen by STEM-EDX. (b) HRTEM of the U-particle. With Wiener-filtered image and FFT, (c) HRTEM images show that U-bearing nanoparticles are encapsulated in the "cage" structure of fulleroid. Reproduced with permission from ref 29. Copyright 2011 Springer-Verlag Berlin Heidelberg.

Microbial-mediated uranium reduction using multispecies bacteria biofilms on biotite was investigated using confocal laser scanning microscopy (CLSM).[40] Formation of uranium particles embedded in the biofilm was observed. Through evaluation of the excitation and emission spectra recorded at U hot spots in the biofilm, the authors detected the presence of U(V) in a multispecies biofilm. This was interpreted as proof

dx.doi.org/10.1021/cr300343c | *Chem. Rev.* 2013, 113, 995–1015

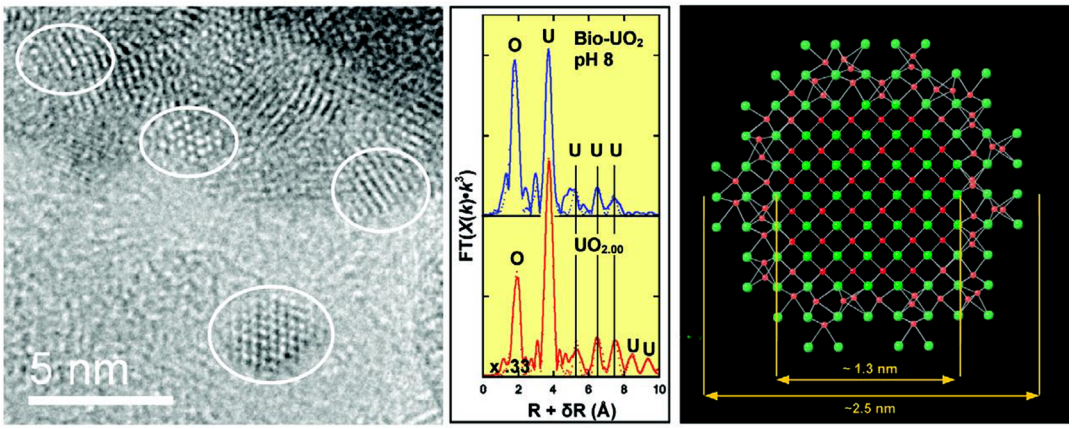

Figure 3. (left) HRTEM image of biogenic uraninite produced by *Shewanella oneidensis* strain MR-1. (middle) EXAFS shows the particles to have an ordered structure. (right) Schematic cross section of a particle, showing inner 1.3 nm core of $UO_{2.0}$, surrounded by a distorted, crystalline outer layer. Reproduced with permission from ref 36. Copyright 2008 Mineralogical Society of America.

that the reduction mechanism is a one and not two electron process.

Although not a report of natural source of actinide nanoparticles, it appears an appropriate place to mention here cell interactions with plutonium. An early (first) review of interactions of Pu and microbes is found in ref 41. A recent investigation of the interaction of mammalian (Pheochromocytoma cells from a rat adrenal gland) cells with Pu was reported by Jensen et al.[42] In cells treated with ^{242}Pu(IV), intracellular Pu hot spots were identified using scanning X-ray fluorescence analysis (μ-XRF) with a submicrometer beam (Figure 4). Differences in the Pu L3-edge micro X-ray

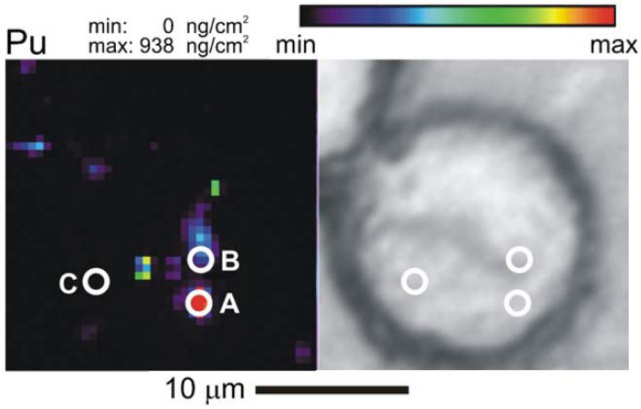

Figure 4. (left) Plutononium distribution map extracted from μ-XRF data for a cell incubated with plutonium aggregates. (right) Corresponding optical micrograph. Circles mark areas revealed by XANES to consist of Pu(IV). Adapted from ref 42. Copyright 2012 Elsevier.

absorption near edge spectroscopy (μ-XANES) white line intensity measured at three different hot spots identified in Pu elemental maps and comparison to results reported in ref 43 indicate that particles of different sizes are associated with the cell.

2.2. "Hot" Particles Released in the Environment

There are different sources of "hot" particle release, most of them due to military use of nuclear energy such as nuclear explosions, cold detonations of nuclear materials, and airplane crashes involving nuclear arms. Research concerning this type of source is covered in section 2.2.1. Uranium particles in the environment stemming from use of depleted uranium ammunition are described in section 2.2.2. "Hot" particles originating from reactor accidents and release from weapons and fuel fabrication and reprocessing sites is treated in section 2.2.3. The special role of colloids in transport of actinide elements in the environment is the topic of section 2.2.4. In all of these sections, the reader should gain insight into the importance of studying both actinide particle isotope content and speciation (physical and chemical form).

Use of modern techniques often allows identification of the source from analysis of a single particle. Only recently, element and isotopic analysis on single nanoparticles became possible due to the availability of mass spectrometric methods operating in imaging mode, SIMS but also laser-ablation (LA) ICP MS (for a comprehensive overview, see ref 10a). Imaging is possible with all kinds of SIMS instruments, however, with strongly varying spatial resolution. Detailed overviews of SIMS techniques can be found in refs 9,44. Standard small geometry SIMS machines achieve resolutions on the order of micrometers, whereas NanoSIMS from Cameca (dynamic SIMS; firm in France) and NanoTOFSIMS (static SIMS) achieve a lateral resolution of less than 50 nm. While the dynamic SIMS continuously ablates material and is well suited for trace analysis and depth profile, static SIMS is employed for investigation of thin surface layers, the sensitivity strongly depending on the instrument. Resonant post ionization of neutrals can strongly enhance the sensitivity of SIMS while maintaining less than 50 nm lateral resolution.[45] In combination with other sophisticated methods with similar resolution, the SIMS isotopic information can be augmented by knowledge of actinide chemical state using complementary techniques so that a comprehensive characterization of submicrometer particles is possible. By these means, for example, solid PuO_2 particles from nuclear explosives can be distinguished from so-called pseudocolloids, that is, actinide containing particles, which carry only a small number of actinide atoms either incorporated into or sorbed onto their surface. In general, radionuclide composition, activity concentration, isotope ratios, and burn-up will reflect the emitting source of released particles, while particle characteristics such as size distribution, crystallographic structure, and oxidation state

ultimately depend on their release scenarios (i.e., affected by temperature and pressure, presence of air) and histories.[46] Volatility of the released material as well as particle characteristics are determinant in "hot" particle ecosystem behavior.[47]

A large portion of radioecological studies focus on measuring isotope ratios of radionuclides, to trace back the origin of the material, but do not further characterize the chemical (or physical) species. Chemical speciation of nanoparticles is possible by use of soft ionization methods such as ESI,[48] which has been recently improved for working in the trace concentration regime.[49] Synchrotron-based (spectro)-microscopy and other techniques providing chemical state and structure/morphology information in recent years are increasingly applied in investigations of micrometer and submicrometer-sized particles.[42,50,51] Collecting radioactive particles on, for example, an air filter, followed by ashing and mass spectrometric investigation yields information concerning isotope content but destroys all traces of chemical and physical form. However, the chemical and physical "speciation" is a major factor affecting actinide particle reactivity/stability and therefore in predicting their behavior in the biogeosphere. This information is available with state-of-the-art spectro-microscopy. In the following sections, the importance of particle isotope content for identification of its source and the equal importance of speciation investigations of actinide containing nanoparticles in the environment are evident in the examples presented. Likewise, the examples illustrate for the reader relationships between structure and stability, physical form and solubility, as well as between speciation and mobility in groundwater.

2.2.1. "Hot" Actinide Particles from Military Nuclear Devices. Actinide containing particles from military use span a size range from submicrometer[47] to several hundred micrometers.[52] Pure An or AnO_x particles (An = Pu,U) and mixtures thereof have been reported. Composition and chemical speciation depend strongly on the conditions of particle release and on subsequent fate of the particles in the environment (for instance, oxidation, weathering, etc.).

Single particle isotope ratios were obtained by combining surface analytic techniques and ICP MS in investigations of particles released from the air plane accidents carrying nuclear warheads near Palomares, Spain (1966) and Thule, Greenland (1968).[50b] Particles were sampled and measured by SEM, micro X-ray fluorescence (μ-XRF), and μ-XANES. From these nondestructive methods, the authors identified intrinsic actinide particles (UO_2, U_3O_8, and plutonium oxides in varying oxidation state) down to 1 μm in size. Single particles were then selected, digested by microwave boiling in HNO_3, and finally the $^{235}U/^{238}U$, the $^{240}Pu/^{239}Pu$, and the ^{235}U /^{239}Pu ratios were determined. Both Palomares and Thule particles contained a mixture of weapon grade plutonium and enriched uranium. The particles from both sites were found to be similar, pointing to the initial release source conditions, and not the environmental conditions during aging for nearly four decades, as the major determining factor of the particle characteristics. Using XRF microtomography combined with μ-XANES, the U and Pu distribution in a Thule particle removed from sediment showed that the f-elements were inhomogeneously distributed (Figure 5) and coated with iron containing material from the sediment. Uranium was found to be mostly tetravalent in the particles studied and particles with two types of Pu species were found, one type with Pu(IV) and the other with a mixture of Pu(IV) and Pu(VI).[53]

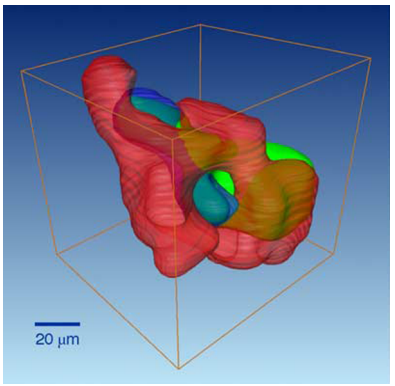

Figure 5. Reconstruction of a Thule "hot" particle from sediment from microtomography data performed at the ANKA synchrotron. Iron (red) from sediment coats Pu (blue) and U (green). Reprinted with permission from ref 53. Copyright 2005 Elsevier.

We note here that precise quantification of minor isotopes such as ^{234}U and ^{236}U and of plutonium isotopes due to isobaric interference are challenges facing isotopic ratio determinations for specifying actinide particle source. In a study reported in ref 54, the authors combined SEM for identification of uranium particles followed by thermal ionization MS (TIMS) and ICP MS measurement on single particles, which were previously selected and transferred onto a silicon wafer using a micromanipulator.[55] Selection and isolation of particles for analysis reduced molecular ion interference, thereby increasing the precision and accuracy of $^{234}U/^{238}U$ and $^{236}U/^{238}U$ determinations, which are indicators for differentiating between natural uranium sources and ^{236}U produced from neutron capture of ^{235}U in chain fission reactions.

Plutonium particles released during above ground nuclear weapons detonations at the Southern Pacific Marshall Islands were analyzed by Jernström and co-workers using electron microscopy, synchrotron-based methods, and SIMS.[50a] The SIMS instrument they used was equipped with magnetic sector analyzers with a mass resolution of up to $m/\Delta m$ = 25 000. This high resolution is particularly helpful for discriminating isobaric molecular interferences. The particles from Runit Island were found to be either composed of pure plutonium or Pu embedded in a Si/O rich matrix. From the rather low $^{240}Pu/^{239}Pu$ ratio measured, the particles were identified as originating from explosions with low fission yields, which were indeed conducted in the vicinity of Runit Island, Enewetak Atoll, between 1946 and 1958.

Hamilton et al. measured plutonium-containing particles from the Fig-Quince zone on Runit Island.[56] Isotopic composition and physical characterization of the particles were obtained, and the highest percentage of radioactivity was observed to be present in the <20 μm fraction. Because these small particles of alpha emitters are potentially very mobile and might be resuspended in the atmosphere as an aerosol, they can be easily ingested or inhaled and thereby pose a long-term health risk (cf., section 5). This finding is not only important for its implications for possible reuse of the land but also for prospective cleanup operations. Some high activity soil particles were observed to exhibit a surface coating, limiting the effects of weathering on the particles and reducing the ability for particle bound radionuclides to interact with the environment.

2.2.2. Nanoparticles from Depleted Uranium (DU). Particles originating from depleted uranium (DU; a byproduct

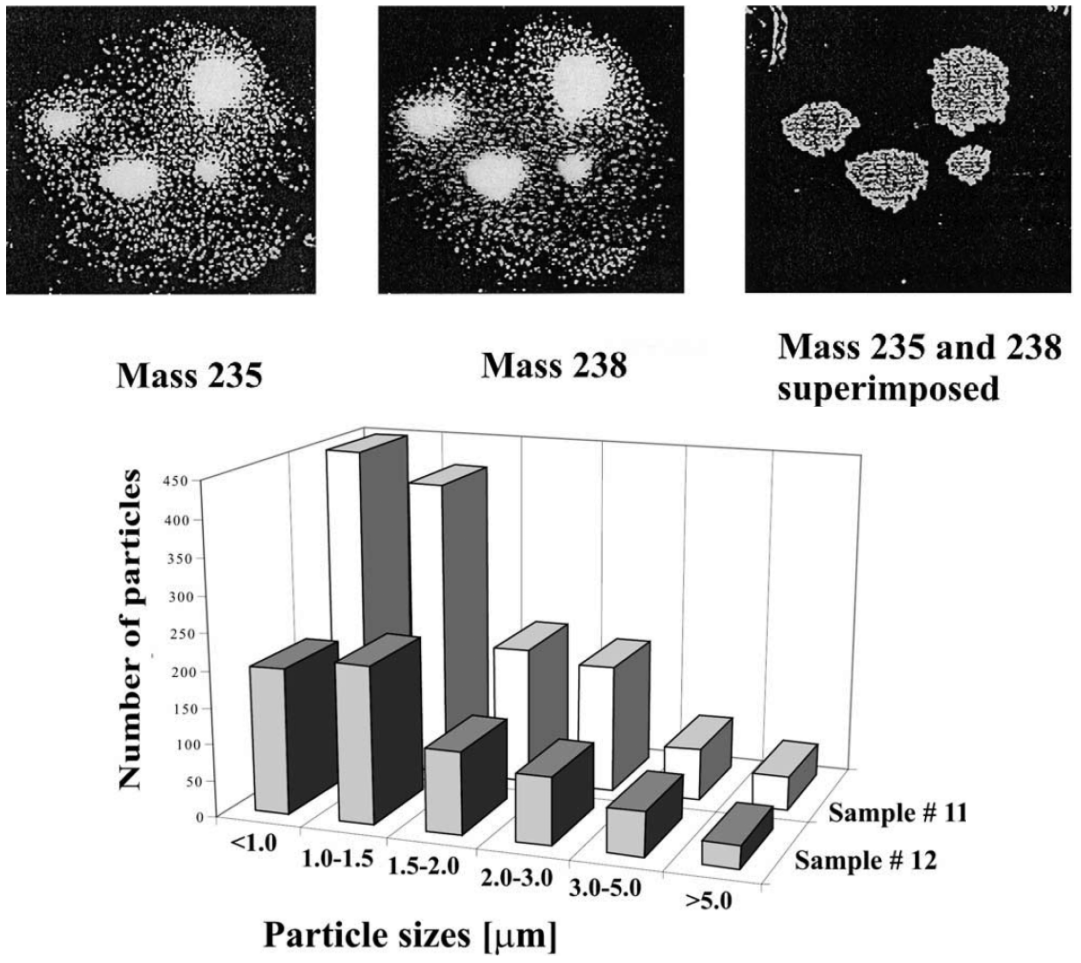

Figure 6. (top) SIMS images for the two uranium isotopes ^{235}U and ^{238}U and for the DU particles. Bottom: Particle size distribution measured by SEM. Reprinted with permission from ref 57. Copyright 2003 Elsevier.

of enriched nuclear fuel production, having less ^{235}U than natural uranium ores) ammunition used in the Kosovo conflict were investigated by Danesi et al. (Figure 6).[57] Samples were suspended in heptane, brought onto a graphite planchet, and measured by magnetic sector field SIMS. All particles under investigations had a isotope ratio $^{235}U/^{238}U \approx 0.002$, corresponding to depleted uranium. More than 50% of the particles were smaller than 1.5 μm, making them potentially harmful to human health because they can be dissolved or resuspended (cf., section 5). Lind et al.[47] determined oxidation state distribution (mean oxidation state of uranium DU particles), indicating strong influence on weathering.

Possible Pu contamination of ammunition used in the Kosovo conflict, potentially resulting from ammunition fabrication using DU originating from reprocessed nuclear material, has received considerable attention.[58] Mass spectrometric detection of Pu in DU ammunition is a great challenge, due to the huge excess of ^{238}U over ^{239}Pu and the isobaric interferences between $^{238}U/^{238}Pu$ or $^{241}Am/^{241}Pu$. Even the high resolution inherent to sector field instruments often is insufficient to resolve the isobars. Bürger et al.[59] measured a total Pu content of ~15 pg/g uranium in the DU ammunition using the highly element and isotope selective RIMS and inferred from the Pu isotope ratios that at least part of the material was reprocessed from uranium previously exposed to a considerable neutron flux. High mass resolution results are reported by Erdmann at al., where they were successful in imaging distributions of the fissile isotopes ^{235}U and ^{239}Pu from inside a warhead (from Thule) and of ^{238}U from the warhead DU outer shielding (Figure 7). The authors also demonstrated that RIMS can be used to post ionize neutral fragments of actinides sputtered by ion bombardment in a SIMS instrument.[52] This promising approach can combine the submicrometer spatial resolution typical for nanoSIMS with the excellent element and isotope selectivity of RIMS.

2.2.3. "Hot" Actinide Particles from Reprocessing of Nuclear Material and Accidents. Much work was performed on "hot" particles released during the reactor accident of Chernobyl, and a comprehensive review was published recently by the IAEA.[5] The influence of temperature and fuel matrices was investigated for particles within the 30 km zone around the Chernobyl Nuclear Power Plant (NPP).[60] The results from these investigations show that crystalline fuel fragments were released during the early stages of the accident (explosion). In contrast, more soluble fuel particles with a UO_2 core and surface layers of oxidized uranium were released during the subsequent fire.[61] The influence of source and particle history on particle solubility due to differences in structure and speciation is evident in studies of particle weathering rate and soil to plant transfer. Isotopes of refractory elements (e.g., plutonium) were released during the Chernobyl accident mainly in the form of fuel particles. The ratio of UO_2 and UO_{2+x} particles in Chernobyl soil fractions were found to determine particle stability against dissolution and release of

dx.doi.org/10.1021/cr300343c | Chem. Rev. 2013, 113, 995−1015

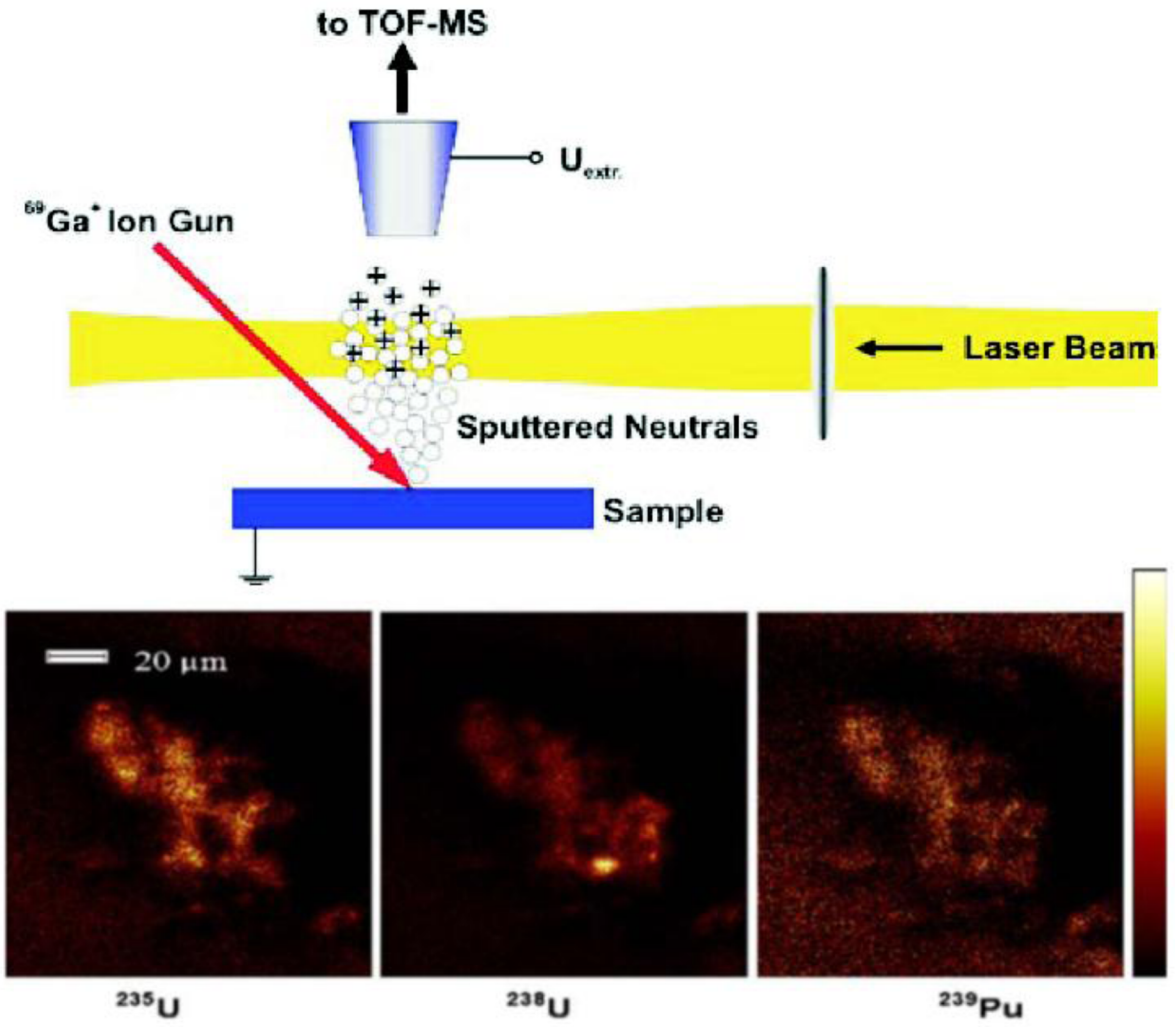

Figure 7. (top) Schematic view of the experimental arrangement for the coupling of ion beam sputtering and resonant laser postionization of sputtered neutrals. For sputtering, a ^{69}Ga ion gun is applied and ions are extracted into a TOF mass spectrometer. (bottom) Lateral distribution of ^{235}U, ^{238}U, and ^{239}Pu in a "hot" particle from Thule, determined by TOF-SIMS. The relative ion intensity in each pixel is visualized by a color scale from black/red (low intensity) to yellow (high intensity). Reproduced with permission from ref 52. Copyright 2009 Springer-Verlag.

uranium and plutonium; higher oxidized fuel particles were observed to be more soluble, and higher soil acidity also promotes fuel particle dissolution; that is, dissolution was slow for particles released during the explosion and high for particles released during the fire.[62] Fuel particles transformation constants were determined and yield initial projections of the role of particulate contaminations as a secondary, diffuse long-term source of actinides.[62a]

The role of actinide containing particles as a long-term contaminant source was discussed by Burns et al.[63] They conclude that for nuclear accidents involving spent nuclear fuel, as was the case for reactor units 1, 2, and 3 of the Fukushima-Daiichi nuclear power plant, uranium nanoparticles, as well as particles containing fission products, may play a crucial role in migration of radioactivity.

A recent publication[64] reported on α-spectrometry and ultrafiltration investigations of groundwater collected near a contaminated trench (containing fuel components and other radioactive waste, humus topsoil, and contaminated vegetation) in the "Red Forest", an area used for shallow disposal in Chernobyl cleanup operations. The results indicated that the trench was the main source of the radionuclides found in the aquifer and that Pu is mobile in the groundwater, moving 5−15 m from 1987 to 2005. Near the source the majority of Pu was present as pseudocolloids, specifically associated mainly with low molecular weight species (<1 kDa). The total amount of Pu and the amount associated with groundwater particulate matter showed variations connected with seasonal fluctuations in the water table. Americium is apparently more mobile than Pu in the aquifer, as indicated from higher ratios between americium and plutonium isotopes in monitoring wells compared to the average value in the fuel component of the Chernobyl fallout.

Radioactive particles have been released from reprocessing plants, for example, in Europe and Russia, during their operation. Release of radioactivity some 20 years ago from the reprocessing plants La Hague and, to a much stronger extent, Sellafield have led to the formation of "hot" particles containing Pu and Am in marine environments;[65] Irish Sea sediments have been found to be contaminated with uranium containing particles.[66] Detailed information of particles released from La Hague, France, is still lacking, but it is known that a major fraction of radionuclides in La Hague and Sellafield

dx.doi.org/10.1021/cr300343c | *Chem. Rev.* 2013, 113, 995−1015

effluent during normal operation was associated with particles and colloids.[66]

Particles containing fission products and actinides were released accidentally at Dounreay, UK, in the mid to late 1960s and early 1970s into the North Atlantic Ocean.[67] Uranium fuel particles from the Materials Test Reactor (MTR) and Dounreay Fast Reactor (DFR) can still be collected on nearby beaches.[68] At a sandy beach close to the plant, ca. 1200 particle fragments of irradiated nuclear fuel have been collected and analyzed to date. These "hot" particles typically contain 15%−25% by weight uranium and variable amounts of Al from the fuel cladding.

Accidental release from radioactive material or intentional dumping onto soil and in surface waters has occurred at a number of civil and military separation plants. Salbu et al.,[69] for example, identified actinide particles in sediments collected near nuclear containers (originating mostly from submarine nuclear reactors) dumped in the fjords of Novaya Zemlya[70] and U fuel particles in the Yenisey River stemming from emissions from Krasnoyarsk Mining and Chemical Combine.[71]

The Rocky Flats Environmental Technology Site was the location of a complex involved in the United States nuclear weapons production for nearly 40 years, which was contaminated with radionuclides from improper storage, accidents, and other incident releases. The Pu and Am activity was found to be in the top 12 cm of soil and often localized in "hot" particles.[72] This information helped in remediation of the site to minimize resuspension and air (aerosol) transport of radioactivity.

Another weapons contaminated legacy site in the United States is the Hanford Site, located on the Columbia River in Washington. The uranium contamination in samples collected from the vadose zone observed using electron microprobe analysis (EMPA) and TEM combined with focused ion beam (FIB) was shown to be concentrated in microphases of phosphates with varying water content and nanophases of poorly crystalline aluminosilicates, amorphous Zr, Fe, or Mn material, and layered phases and coatings associated with basaltic glass and clasts. Slow kinetic release from and exchange in and out of these nanomaterials during varying groundwater levels may play an important role in the persistence of the groundwater U-plume at this site.[73]

Giere et al.[74] measured aerosol uranium containing particles deposition on cypress leaves collected at locations close to the nuclear facility Malvési located in southwestern France. The particles were found to be composed of uranium oxide, suggesting their originating from fuel fabrication. However, also some uranium-oxide-fluoride particles were found, indicating a likely release of uranium hexafluoride, UF_6, used in gaseous diffusion enrichment. Solid uranyl fluoride (UO_2F_2) can be generated in the atmosphere upon reaction of UF_6 gas with atmospheric water vapor:[75] UF_6 (g) + $2H_2O$ (g) → 4HF (g) + UO_2F_2 (s).

We have mentioned that weathering of actinide containing particles is an important source term. This has been addressed in a model study of the weathering behavior of nuclear fuel reported in ref 76. The authors developed a chamber for studying UO_2 alteration under radiolysis of surrounding water in situ with Raman spectroscopy. They could show direct evidence for the development of studtite ($[(UO_2)O_2(H_2O)_2]\cdot 2(H_2O)$) and schoepite ($((UO_2)_8O(OH)_{12}\cdot 12(H_2O)$) layers known to form as secondary phases at the UO_2/H_2O interface under oxidizing weathering conditions at acidic pH.[77] That studtite particles form under conditions with higher peroxide concentrations (instead of schoepite without peroxide) was then demonstrated in a Raman microspectroscopy study[78] and later by XRD.[79]

Not just weathering and the interplay of dissolution and secondary phase formation, but also sorption of actinide particles onto surfaces in the geosphere determine actinide mobility. In recent years. the interaction of actinide containing nanoparticles with mineral surfaces has been intensively investigated, because their sorption behavior and/or complexation equilibrium constants potentially differ considerably from those of the respective mononuclear ions. Arnold et al. investigated uranium(VI) nanocluster (1−2 nm) sorption onto muscovite using time-resolved laser fluorescence spectroscopy (TRLFS) and HAAD-STEM. Two species were distinguished on edges of muscovite, one a molecular species and the other an amorphous U(VI) condensate of nanosized clusters of polynuclear uranyl(VI) surface species with a particle diameter of 1−2 nm.[80] Schmidt et al.[81] investigated sorption of preformed Pu(IV) nanoparticles ($[Pu_{38}O_{56}Cl_x(H_2O)_y]^{40-x}$ colloids described in ref 82) on muscovite by crystal truncation rod (CTR) and resonant anomalous X-ray reflectivity (RAXR) measurements. The Pu(IV) nanoparticles were observed to sorb to 17% of the surface by strong electrostatic interaction and by partial aggregation of the nanoparticles above the sorbed layer.

2.2.4. Colloid-Mediated Transport. Colloid-mediated transport (or colloid facilitated transport) of actinide elements is an important pathway in migration of these elements in the geosphere[83] (see Figure 8). Colloids mobile in groundwater are known to "carry" or transport contaminants in the aquifer. This is reflected in the observation that, in breakthrough curves of column tracer studies, contaminants associated with colloids sometimes travel faster through porous geological media than the conservative tracer used.[84,85] This is explained through exclusion chromatographic effects within the column. A pioneering work reported by Kersting and co-workers[86] revealed the importance of colloid-mediated transport in actual groundwaters located close to the nuclear bomb test sites in Nevada, where surprisingly high amounts of Pu and fission products were observed to be associated with the groundwater colloid fraction. These authors combined filtration experiments, followed by a ultrasensitive low-ionization MS technique (surface ionization-diffusion-type) for determination of $^{239}Pu/^{240}Pu$ ratios for each size class, with XRD and SEM. The authors identified the source from the isotopic ratios and determined that the radionuclides had migrated at least 1.3 km over a period of about 30 years. They concluded that the extraordinary mobility of the Pu was explained by colloidal transport, possibly adsorbed onto clay colloids or as intrinsic colloids, as the Pu concentration observed in groundwater samples was not found in dissolved form, as expected from solubility data; rather Pu was associated with the filterable fraction. Subsequent TEM (HAADF-STEM, SAED, HRTEM) and EDX investigations revealed the actinide U to be present in colloid form, associated with Cs, silicates, and as a oxide hydrate (Pu was below the detection limit).[87] Similar effects were observed downstream the reprocessing plant of Mayak, investigated by Novikov and co-workers.[88] By means of SEM microprobe analysis, HAADF-STEM, and nanoSIMS, single colloids were imaged, and plutonium was found to sorb most efficiently onto amorphous iron hydroxide colloids.

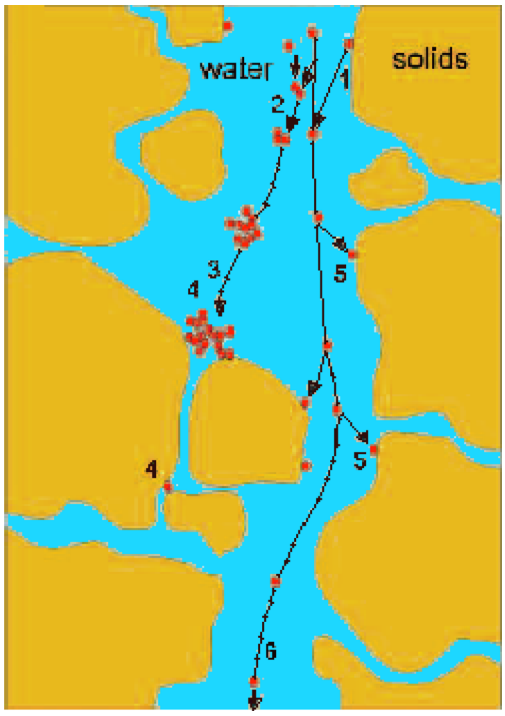

Figure 8. Processes controlling the mobility of colloidal particles as potential carriers of contaminants, including actinide elements, in water-saturated porous media: (1) release of colloids, (2) aggregation of colloids, (3) immobilization by gravitational settling of floccs, (4) immobilization by constraining floccs or single particles, (5) immobilization by colloid deposition on solid−water interfaces, and (6) transport of dispersed colloidal particles (and their contaminant burden) over long distances by flowing water through the larger pores, being excluded from the smaller ones. Reproduced with permission from ref 213. Copyright 2005 Mineralogical Society of America.

An alternative approach was pursued by Dai et al.[89] who investigated colloid-mediated transport at the Savannah River site. Plutonium and transplutonium isotope distributions were measured by TIMS, allowing exclusion of global fallout as a possible source and tracing back the Pu origin to nuclear reactor production. Note that while TIMS is well suited for ultra trace detection, it requires quite extensive pretreatment of the sample. In the case of Dai et al.,[89] nanoparticles were separated from ionic species out of several kilograms of sample by cross-flow ultrafiltration, subsequently coprecipitated with LaF_3, dissolved in 7.5 M HNO_3, separated several times in exchange columns, and eluted into AG1 × 4 mesh resin. Furthermore, no single particle measurements are possible without pretreatment and information by additional techniques. It is interesting to note that Dai et al. interpret the presence of Pu isotopes downstream from the source basin of their study in a scenario different from the colloidal transport of Pu in the Nevada test site and Mayak, as in the particular groundwater investigated <4% Pu was found colloid bound. They observed elevated $^{240/239}$Pu ratios furthest from the source, suggesting transport of ^{244}Cm, which was also produced at the site, and progeny ^{240}Pu in-growth from ^{244}Cm decay (half-life = 18.1 years).[89]

Because of colloid-mediated transport, contamination by actinide bearing particles is an issue not only limited to areas in the immediate vicinity of sources such as the reprocessing plants Sellafield and La Hague.[90] Plutonium may be released in ionic form, presumably as Pu(IV) or Pu(V) depending on pH and Eh conditions. Suspended particles and colloids act as efficient transport carriers of transuranics introduced to surface waters to sediments.[91] This is known to have taken place in the Irish sea[92] (so-called "mud basin") and confirmed by Zheng and co-workers to also be the case in the Northwest Pacific. By means of ICP MS, plutonium was determined to originate only partly from global fallout and partly introduced directly from the Pacific Proving Grounds (nuclear test sites of the 1940s to 1960s).[91]

Colloid facilitated transport remains one of the largest uncertainties in quantifying future dose levels in the analysis of the long-term safety of deep geological repositories for nuclear waste. Actinide containing (nano)particles can originate from dissolution of the waste forms following groundwater intrusion into a repository and corrosion/breaching of the multiple barriers. Buck et al. investigated colloid formation from vitrified wastes.[93] Colloidal and suspended glass alteration particles present in leachates of these tests were examined with analytical transmission electron microscopy (AEM). Typically a U:Si ratio of 1:3 was observed. Depending on the conditions and aging, both amorphous uranium silicate particles and crystallized uranium silicate colloids were present. In a previous study, Kim et al. observed Pu colloid formation from leaching of waste glass.[94] These Pu nanoparticles show optical absorption, which is surprisingly similar to the one of synthetic $[Pu_{38}O_{56}Cl_x(H_2O)_y]^{40-x}$ colloids made by Soderholm and co-workers.[82] In ref 95, a number of factors and processes contributing to colloid stability were analyzed and reported that coating of actinide bound colloids with natural organic material, as well as kinetic stabilization of their binding, likely play an important role in colloids ability to serve as vehicles for actinide transport.

A recent survey of the potential capacity of aquatic (clay, metal hydroxides, silica, and silicate) colloids originating from sediments from Lop Nor, a former nuclear test site and one of the proposed high-level waste sites in China, for transporting actinide radionuclides (as pseudocolloids) and comparison to the mobility of intrinsic Pu(IV) colloids recently appeared in the literature.[96] Addition of sodium ions reduced the stability of the pseudocolloids; this was, however, observed to be a transient effect.

Highly charged actinide ions undergo strong complexation reactions in solution. In many cases, complexation is the first step toward formation of polynuclear species and polymerization to nanometer-sized entities in solution. One example is the complexation by citric acid relevant for final disposal of radioactive waste in the Waste Isolation Pilot Plant, WIPP (Carlsbad, NM). The solution complexes of Pu(IV), which form in the presence of excess citric acid,[97] include, in addition to mononuclear species, dimeric citrate complexes, $[Pu_2(Hcit)(cit)(H_2O)_4(OH)_2]^+$ (cit denotes $C_6H_5O_7^{3-}$), which were characterized using XANES and EXAFS. Biodegradation of the Pu citric acid complexes by *Pseudomonas fluorescenes* bacteria induced polymerization of Pu(IV), i.e., formation of small plutonium nanoparticles between pH 0 and pH 4.

3. AEROSOLS/SAFEGUARDS

The technical feasibility of tracking the origin of single "hot" particles makes them ideal candidates for nuclear safeguard operations. Measuring isotope ratios of bulk samples runs the risk of averaging contributions of different sources. This is not the case for single particles. Furthermore, one avoids misinterpretation due to admixtures of radiosiotopes from

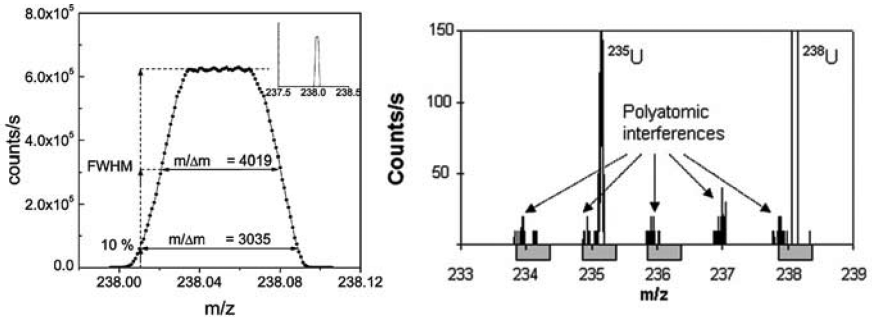

Figure 9. (left) Example of peak shape of ^{238}U obtained with a Cameca 1270 SIMS. Mass resolving power ($m/\Delta m$) at full width half-maximum and at 10% of peak height is given. (right) A mass scan from a U particle from a swipe sample displaying additional polyatomic peaks at $m/\Delta m$ 3035. The gray rectangles represent the width of the uranium peaks at $m/\Delta m$ 450; normal working conditions for SG-SIMS instruments on nuclear swipe samples. Reproduced with permission from ref 103. Copyright 2009 The Royal Society of Chemistry.

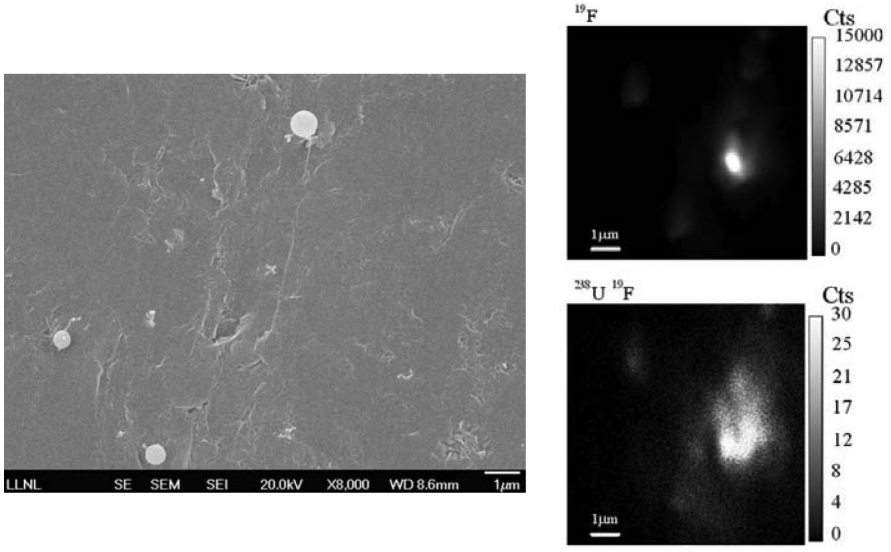

Figure 10. (left) Scanning electron microscope image of a UO_2F_2 particle sample prepared at the IRMM (Institute for Reference Materials and Measurements, Geel, Belgium) showing the particle distribution on the graphite planchet. Scale bar is 1 μm. (right) Ion images for $^{19}F^-$ and $^{238}U^{19}F^-$ (9 μm × 9 μm) obtained by NanoSIMS 50 showing a uranium oxyfluoride particle (bright spot). Reproduced with permission from ref 104. Copyright 2009 Akadémiai Kiadó.

omnipresent background such as global fallout. While fission track analysis after neutron irradiation provides a fast method to gain a crude estimate of particle size and enrichment,[98] more detailed information is obtained by mass spectrometry. In ref 99, fission track analysis was combined with TIMS for the investigation of single uranium bearing particles of swipe tests. Nowadays, SIMS analysis of $^{235}U/^{238}U$ ratios in aerosols from swipe samples is a most powerful and versatile tool to detect undeclared nuclear operations in reprocessing or fuel fabrication plants.[100] Following detection and separation of single particles, Zhang and co-workers successfully measured the uranium isotope ratios of individual particles for nuclear safeguard purposes.[101]

In a further study, the age of PuO_2 particles was studied as a potential method for validating compliance to the Fissile Material Cut-off Treaty for nuclear weapons material. For bulk material, the $^{241}Am/^{241}Pu$ ratio is routinely determined by γ-spectroscopy and used for age determination. However, the tiny amount of γ emitters in single nanoparticles inhibits use of this method. By SIMS, the ratios of $^{238}Pu/^{234}U$, $^{239}/Pu^{235}U$, and $^{240}Pu/^{236}U$ were measured and evaluated[102] to give precise information on the age of particles without need for chemical separation or pretreatment. The feasibility was first demonstrated on well-defined PuO_2 particles from a Round Robin test and applied to study a PuO_2 sample confiscated at Munich airport in 1994.[102]

On the basis of the atmospheric process mentioned in section 2.2.3, UF_6 release and subsequent formation of UO_2F_2 nanoparticles, production plants are tested for undeclared operation such as fabricating highly enriched uranium by determining the isotope ratio of single particles, making use of highly accurate mass spectrometry. Ranebo et al.[103] discussed advantages of large geometry LG-SIMS versus TIMS after fission track analysis and included discussion of resolving power needed to overcome most common molecular isobaric interferences (Figure 9). The F to U ratio was determined on the 50−100 nm scale by nanoSIMS, which allows one to probe source terms and age of individual particles.[104] This investigation was particularly challenging due to the large mass difference of U and F, requiring for sensitivity calibration of the mass analyzer over a wide mass-overcharge range (Figure 10).

4. SYNTHETIC PARTICLES

4.1. Reference Actinide Particles

It is obvious from the previous chapters that high precision measurements of isotope ratios require quality assurance and quality control of the methods by use of certified reference materials. Consequently, sources of actinide nanoparticles with well-defined isotopic composition are needed.[105] There are several possible processes and strategies for producing such well-defined reference particles. For example, actinide particles can be produced from bulk material by breaking and milling. In contrast to environmental samples, particles produced in the lab can be monodisperse. Although this might render them poor models for studies to mimic behavior of heterogeneous actinide particles, such synthetic monodisperse samples can serve well as reference material. Varga produced nanoparticles from uranium oxide powder and measured isotope distributions of single uranium particles by LA ICP MS.[106] The particles were deposited on double sided tape on a cardboard holder and vaporized by a 213 nm YAG laser. The ablated material was carried into the plasma by argon carrier gas. Depleted, natural, low enriched, and highly enriched uranium particles were characterized with respect to their ^{234}U, ^{235}U, ^{236}U, and ^{238}U content with typical precisions of 1−5%. The authors pointed out the need for reducing molecular interference by operating the instrument at high mass resolution (SF MS), which is particularly important for investigating small particles and to increase accuracy in the quantification of minor isotopes.

Monodispersed micrometer-sized uranium particles have been produced from reference material.[107] As many "hot" particles also contain plutonium, the method was adapted to produce standard particles containing plutonium and uranium/plutonium mixtures with different U/Pu ratios.[108] The method used consisted of a vibrating orifice aerosol generator system, equipped with a furnace system for calcination of the actinyl nitrate aerosol particles generated. The system was implemented within a glovebox for radiological safety. Certified isotope ratios were reproduced within 1−8% statistical error by measuring single particles using a double focusing sector field SIMS optimized for fast switching between masses to be analyzed.

A very recent example of the synthesis of U and Th oxide nanoparticles prepared by reaction of metal cation acetylacetonate in dibenzyl ether at 280 °C, using various stabilizing agents such as oleic acid to prevent extended oligimerization/agglomeration, appeared in ref 109. The authors were successful in synthesizing ThO_2 and hyperstoichiometric UO_{2+x} with consistent morphology and small size ranges. Analysis with TEM and HRTEM showed the uranium product to be isotropic faceted nanodots 3.6 ± 0.4 nm in size. The thorium synthesis led to the formation of nanorods.

Well-defined systems can be used for method development and quality control. For example, the application of fully automated scanning of a large number of particles on a substrate is possible by use of large geometry SIMS, which was demonstrated recently on monodisperse uranium oxide particles produced by the method described in ref 103. A more novel application of well-defined nanoparticles is the application of ThO_2 nanoparticles as a stain with high Z-contrast in SEM/TEM investigations of bacteria and other microorganisms and their associated lipopolysaccharides.[110]

The precision up to which isotope ratios can be measured depends obviously on particle size. One hundred nanometer-sized particles contain only some 10^8 atoms, making precise determination of minor isotopes a real challenge. Esaka et al.[100] proved in a study on certified uranium reference material that a precision of 10% or better can be achieved for SIMS investigations on single submicrometer particles, even for the low abundant isotopes ^{234}U and ^{236}U ($^{234}U/^{238}U = 3 \times 10^{-4}$, $^{236}U/^{238}U = 5 \times 10^{-4}$, corresponding to only about 1 fg). In an investigation of certified plutonium material in the form of particles in tests for quality control of Pu particle analysis in nuclear safeguards and forensics, especially for the determination of Pu isotopic composition and age dating of single Pu dioxide particles, TIMS results showed no significant difference from expected values. ICP-MS and α-spectrometry were used to successfully model in-growth of ^{241}Am from ^{241}Pu with time (up to 674 d).[111]

4.2. Actinide Nanoparticles in Solution

The presence of intrinsic actinide particles in groundwater (also "eigencolloids"), the formation of which is associated with actinide solubilities, can serve as vehicles for actinide transport under conditions one might otherwise expect for precipitation and immobilization, in a manner analogous to pseudocolloids (section 2.2.4). Depending on size, actinide particles or colloids have a strong influence on solubility itself. The smaller is the particle, the higher is the apparent solubility (Schindlers equation[112]). Vice versa, unexpected high solubilities of Th[113] and Pu[114] were successfully explained by the presence of colloids of approximately 2 nm. Because of their high potential for facilitating actinide migration in the environment, much research on the formation, stability, and behavior of actinide eigencolloids has been reported. This section presents research results reported for thorium, uranium, neptunium, and plutonium eigencolloids, preceded by a discussion of their in situ detection.

4.2.1. Detection of Actinide Particles in Solution. Detection of particles in solution is often performed by absorption spectroscopy,[115] static or dynamic light scattering,[116] or, for small colloids <50 nm down to ppt concentrations, by laser-induced breakdown detection (LIBD).[117] Element analysis and characterization of morphology is performed after particles deposition onto a substrate by means of methods used for "hot" particle analysis. The initial step in actinide nanoparticle formation (i.e., formation from molecules), however, is best observed by soft ionization techniques such as MALDI or ESI.[118] So far, only the latter was applied for investigation of actinide polymers.[13,115c,119]

A simple reference material in liquids for calibration and quality assurance can be prepared by suspending dry particles in solution. Actinide nanoparticles suspended in solution (colloids) were investigated by Degueldre et al.[120] A stock solution was prepared by milling commercially available thoria powder with an initial grain size of several μm. These particles were suspended in Milli-Q water. The resulting sample was diluted until the nanoparticle number density ranged from 10^5 to 10^6 mL^{-1} and subsequently introduced into the nebulizer of the ICP MS instrument by a syringe pump slowly, to guarantee that at most one nanoparticle entered the plasma plume at all times. Clear peak structures at masses 232 amu ($^{232}Th^+$) and 248 amu ($^{232}Th^{16}O^+$) allowed the detection of single nanoparticles and also measurement of their size by evaluating the peak area. Correlating the results with SEM, the measurements indicate a lower detection limit of 80 nm nanoparticle diameter. A similar study was performed on

dx.doi.org/10.1021/cr300343c | Chem. Rev. 2013, 113, 995−1015

uranium particles obtained by milling of UO_2 powder.[121] In this case, the signals at masses 235, 238, and 254 amu ($^{238}U^{16}O^+$) were used for nanoparticle size analysis. In addition to a lower detection limit at around 100 nm, the authors discuss also an upper limit of around 5000 nm caused by the finite residence time of the particles in the plasma torch. Larger particles cannot be fully vaporized, which leads to a decrease in signal and underestimation of their size.

Actinide nanoparticles form in aqueous media directly by metal ion hydrolysis, subsequent polymerization, and further growth to form nanoparticles. These are often referred to as (aquatic) colloids if they are sufficiently small to remain suspended in solution. For example, in 0.5 M hydrochloric acid, about 50% of the Pu(IV) is hydrolyzed from Pu^{4+} to $Pu(OH)^{3+}$.[122] With increasing pH, further hydrolysis leads to formation of mononuclear ($Pu(OH)^{4-y}_y$) and at concentrations [Pu(IV)] > 10^{-6} M[123] to polynuclear ($Pu_x(OH)^{4x-y}_y$) complexes, which can grow into nanometer-sized colloids.[124] Such hydrolysis processes forming polynuclear species, polymers, or colloids in aqueous solution are observed for tetravalent ions Th(IV),[113a,125] Pu(IV),[43,125d,126] U(IV),[127] Np(IV),[128] Pa(IV), and Pa(V),[129] and to a lesser extent for the hexavalent actinyl ions U(VI)[127a,130] and Pu(VI).[131,132]

4.2.2. Thorium Colloids. There are a considerable number of studies on Th(IV) polymerization. Two recent reviews summarize available data on physics and chemistry of thorium[133] and solution chemistry of thorium compounds.[134] It is not advisable to use Th(IV) as an analogue for Pu(IV) with respect to studies aimed at elucidating the mechanism of polymerization processes, because there are pronounced differences between the two cation types. In acidic aqueous solutions, Th forms tetravalent ions, Th^{4+},[133] which are slightly larger than Pu^{4+} ions ($r(Th^{4+})$ = 1.0 Å,[135] 1.08 Å;[136] $r(Pu^{4+})$ = 0.96 Å[137]) and are 10-fold coordinated (experimentally determined coordination number = 10.8).[133,138] Because of the ionic radius size difference, formation constants of mononuclear Th(IV) hydrolysis complexes are considerably smaller.[136] The solubility of the amorphous hydroxide exceeds the values of the respective solids of Pu.[113c,134,136] Over the past decade, detailed investigations on the colloid formation mechanisms of Th(IV) revealed that at least two regions with respect to pH and Th(IV) concentration can be distinguished,[133] which correspond to different solid phases, microcrystalline and X-ray amorphous (log $K_{sp}°(ThO_2(microcrys))$ = −52.8[136] to −53.0,[134] log $K_{sp}°(Th(OH)_4(am;hyd))$ = −47.8).[136] At high acidity (pH < 4), microcrystalline colloids form from oversaturated solutions,[113a,b,139] whereas at higher pH Th(IV) colloids form that are X-ray amorphous,[125a] that is, either present as an amorphous hydroxide phase or consist of aggregates of small microcrystalline subunits, most likely with a hydrated surface layer.[125e] The latter assumption is corroborated by a model, where the different solubilities of "crystalline" ThO_2 and "amorphous hydrated" $Th(OH)_4$ are attributed to the presence of particulates (nanoparticles) in the solids,[113b,133,134,140] and the increase in solubility is explained by a decrease in particulate size.[112] It is a surprising fact that solutions that are considerably oversaturated with respect to the solubility of crystalline ThO_2 are stable for years without any tendency toward precipitation, as long as the solubility of the amorphous $Th(OH)_4$(am;hyd) is not exceeded. Th(IV) colloids are stable over long time periods,[113c] and, in analogy to the "fresh Pu(IV) colloids", they are in equilibrium with Th(IV) ions.[141] Reversible formation and dissolution of amorphous thorium oxo hydroxide ("Th$(OH)_4$(am)") colloids proceeds on time scales of a few days.[125b] Colloid formation is preceded by formation of polynuclear hydroxide complexes[124b,135,142] such as $Th_2(OH)_2^{6+}$; $Th_2(OH)_3^{5+}$; $Th_4(OH)_8^{8+}$; $Th_4(OH)_{12}^{4+}$; $Th_5(OH)_{12}^{8+}$; $Th_6(OH)_{14}^{10+}$; and $Th_6(OH)_{15}^{9+}$,[133,136] which, in contrast to the polynuclear complexes of Pu(IV), are accepted as thermodynamically stable species.[134]

4.2.3. Neptunium and Uranium Colloids. Comprehensive reviews on Np aqueous chemistry are available;[143] however only few studies focus on Np(IV) colloid formation. Neck et al.[128] investigated formation and stability of neptunium hydroxide colloids by a combination of laser photoacoustic spectroscopy[144] and laser-induced breakdown detection.[117a,b] In ref 145, attempts were made using a 100 nm-sized X-ray beam to image Np(IV) particles shown to form in microfissures of a granite bore column during a tracer experiment via reduction of Np(V) and precipitation of Np(IV) hydrolysis product.[146]

Similar to known polynuclear cation−cation interaction (CCI) compounds for Np(V),[147] recently interesting U(V) multidentate clusters and polymeric species exhibiting CCIs have been reported;[148] an example of a U(V)-tetramer is shown in Figure 11. The U(V) polynuclear species are not stable in solvents, and use of the U(V) tetramers as ideal compounds as models for investigations of the mechanism of disproportionation reactions has been suggested.[149]

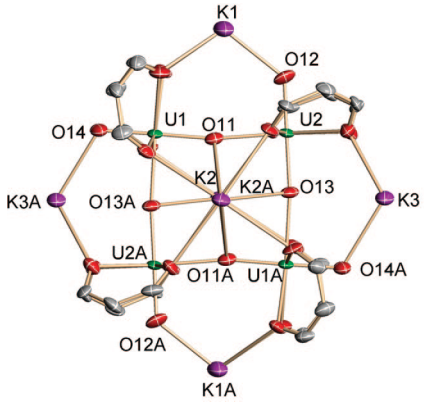

Figure 11. The tetrameric cluster in $\{[UO_2(dbm)_2]_2[\mu\text{-}K(Py)_2]_2[\mu_8\text{-}K(Py)]\}^{2+}$ exhibiting the T-shaped cation−cation interaction. Reprinted with permission from ref 148a. Copyright 2008 American Chemical Society.

Tetravalent uranium shows also a high tendency for hydrolysis and polymerization,[127a,150] and colloid formation was investigated in ref 127b. Under aerobic conditions, hexavalent uranium is more relevant. In contrast to plutonium, polymerization of hexavalent uranium[130d,151] proceeds without bacterial digestion of citrate. Somogyi et al. investigated complexation of uranyl ions with citric acid[152] and detected polynuclear complexes of the general formula $[(UO_2)_n(Hcit)_2(cit)(HNO_3)_p(X)_q(H_2O)_r]^+$, X = $[Na^+;K^+]$. This study was performed using two different ESI ion trap instruments. One is a so-called 3D trap (RF, radiofrequency, or Paul trap), while the second one is a high resolution FT ICR trap (Penning trap). The paper includes a detailed investigation on ion gas-phase reactions, which proceed particularly fast during storage in the 3D trap due to elevated residual gas

dx.doi.org/10.1021/cr300343c | Chem. Rev. 2013, 113, 995−1015

pressure. By successive association steps, $[(UO_2)_nO_m]^-$ nanoparticles formed.

Uranyl polymerizes also in the absence of organic ligands. In combined ESI and time-resolved laser induced fluorescence (TRLIF) studies, mono- and polynuclear uranyl hydroxide complexes were observed.[130a,b] The authors pointed out that combining the complementary techniques TRLIF and ESI MS is particularly helpful. TRLIF is highly sensitive but limited to investigation of fluorescing metals, whereas ESI MS is less sensitive but can be applied to any element and provides direct information on the stoichiometry of the complexes.[153] A study reported in ref 154 observed hydrolysis of uranyl monomers and formation of polymers $[U_mO_{2m}(X,Y)_{2m-1}(H_2O)_n]^+$; (X,Y = OH^-, NO_3^-; $m < 5$) in acidic solutions over a wide concentration range of $[U]_{tot} = 10^{-8}-10^{-2}$ M. Although the unambiguous identification leaves no doubt that the polynuclear species formed in solution, the authors did not measure pH, which precludes use of these findings for calculating equilibrium constants. However, the authors discussed the risk of potential artifacts caused by up-concentration effects using high flux electrospray sources (typically >5 μL min^{-1}). A nanoelectrospray study at lower concentration circumvented these artifacts and quantified dimeric and trimeric complexes in near neutral solutions.[130c]

4.2.4. Plutonium Nanoparticles. *4.2.4.1. Detection of Pu Colloid Oxidation State.* While the oxidation states of Pu are easily distinguished by absorption spectroscopy, this is not true for hydroxide complexes[115a] (cf., ref 155). However, Pu(IV) polymerization leads to alterations in redox equilibria and additional easily identifiable spectral features[156] around 620 nm,[124e] which become more pronounced for aged solutions. This 620 nm peak is evidence for the presence of small Pu(IV) colloids. Absorption spectra of Pu(IV) colloids as a function of age[115b,157] and the method of preparation[115b,158] have been published. For small polynuclear complexes containing only a few Pu ions, no absorption spectra have yet been published, and it is possible that these do not absorb visible light.[117b,159] The oxidation state of Pu can also be determined using Pu L3 XANES.[160]

4.2.4.2. Formation Processes of Pu Colloids. Much of the early work on plutonium solution chemistry was driven by the requirement to separate and purify Pu in highly acidic solutions,[124g,161] and for this application Pu polymers were unwanted species.[124a,162] Some early attempts were made to characterize the polymers.[124b,157,163] Great progress has been made during the last two decades, following recognition of the relevance of Pu colloids for migration and hence for assessment of repositories for nuclear waste.[94,124g,142b,164] Despite their importance, equilibrium formation constants for polynuclear hydroxide complexes are still scarce.

The presence of very small Pu colloids or polynuclear species can lead to enhancement of observed apparent solubility by up to 2 orders of magnitude, depending on pH. The solid phase involved has an effect as well; observed values range widely from amorphous Pu(IV) hydroxide (log $K_{sp}^{\circ}(Pu(OH)_4(am;hyd)) = -58.33 \pm 0.52$)[127a] (cf., much higher solubility reported in ref 165) to crystalline PuO_2 (log $K_{sp}^{\circ}(PuO_2cryst) = -64.0$).[123,136] The formation process of Pu(IV) polynuclear complexes, however, remains a subject of debate. Their existence is, however, generally accepted,[124d,135,141,158b,166] and it is assumed that formation processes involve hydroxide or oxygen bridging of ionic Pu nuclei.[141] The authors of two reviews[127a,167] do not consider Pu(IV) polymers as stable species, but rather reaction intermediates, and claim that colloid formation starts from mononuclear hydroxide complexes ($Pu(OH)_y^{4-y}$). In contrast, Toth et al.[158b] suggested a two-step mechanism of colloid formation, in analogy with the behavior of Th(IV).[133,141] They proposed that small polymeric species such as the Pu trimer form, and after an induction period, which depends on the degree of oversaturation of the solution,[168] colloids grow rapidly. In acidic solutions (pH 0.4–1), an increase in weighted mean colloid size from 12 to 25 nm with increasing degree of oversaturation with respect to amorphous Pu(IV)hydroxide was observed. This is much larger than the 2 nm mean size of crystalline PuO_2 colloids that form in highly concentrated solutions[115b] or at high acidities (1.2 M HCl).[164] Such colloids might be composed of small crystalline subunits covered by an amorphous hydroxide layer in analogy to Th(IV) colloids[125e] (cf., section 4.2.3)

The presence of a constant colloidal Pu(IV) level ($[Pu]_{coll} = 10^{-9}$ M) at pH 7 was explained by formation of chainlike polymers[169] via aggregation of cubic $Pu(OH)_4(H_2O)_z$ subunits and subsequent dehydration, leading to formation of hydrated PuO_2. On the basis of LIBD combined with XAFS investigations, this model was extended[43] for describing the formation of colloids in acidic solutions. At acidic conditions, pH < 2, the Pu(IV) dihydroxo complex dominates in solution[126,136,162,170] with eight to nine coordinating water molecules/hydroxide ligands, at a mean 2.38 Å Pu–O bond distance in agreement with expected values.[171] These cubic ($[Pu(OH)_2(H_2O)_6^{2+}]$) monomers form edge-sharing dimers, trimers, and larger polynuclear complexes by hydrolysis and the condensation reaction $2OH^- \rightarrow H_2O + O^{2-}$, whereby oxide bridge links are formed. Further condensation of ($[Pu_xO_y(OH)_{4x-2y}(H_2O)_z]$) polymers culminates in the formation of large colloids with an ordered Pu–O–Pu backbone fcc (face-centered-cubic) structure. The general schematics for an example of such a condensation between two hypothetical polymers of general formula $Pu_xO_y(OH)_{4x-2y}(H_2O)_{2x+2+y}$ (an edge-sharing dimer with a trimer) to form a polymeric species with O^{2-} bridge links is shown in Figure 12. The condensation of three dimers to maximize the number of shared polyhedral edges would yield a hexameric species with the metal cations arranged in an octrahedral fashion. The actual mechanism can involve hydrolysis with subsequent condensation, condensation of charged species followed by release of protons, or any combination thereof. The highest degree of order is expected for larger clusters with the highest degree of condensation, correlated to the greatest degree of O^{2-} bridging in the resulting cubic network (cf., the solid-state structure for

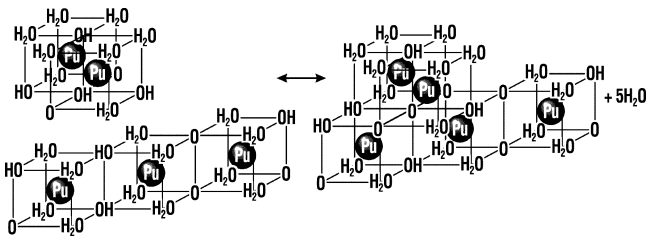

Figure 12. Schematic representation condensation of a $Pu_xO_y(OH)_{4x-2y}(H_2O)_{2x+2+y}$ dimer and trimer to form a larger polynuclear species.

dx.doi.org/10.1021/cr300343c | Chem. Rev. 2013, 113, 995–1015

$Li_{14}(H_2O)_{20}[Pu_{38}O_{56}Cl_{54}(H_2O)_8]$ reported in this issue and in ref 82).

4.2.4.3. Properties of Pu(IV) Colloids. Clearly, it is an oversimplification to speak of Pu(IV) colloids in general terms. Structural investigations over the last three decades indicate that the colloids in rather concentrated and highly acidic media[115b,166a,b] differ from those at higher pH.[172] Fast neutralization of Pu(IV) solutions with a base or water usually leads to formation of less ordered structures;[173] the number[174] and size of colloids formed depend on the growth rate (reaction limited aggregation).[124f] If crystallization germs are present, for example, if Pu(IV) solutions are "seeded" by addition of aged polymers, the colloid formation rate is significantly enhanced[124d] and the size of Pu(IV) colloids formed ranges from a few nanometers[115b,124b] to almost micrometers,[175] depending on the conditions of generation. The colloid density is slightly lower than the density of PuO_2.[176] The colloid morphology seems to vary strongly depending on the conditions of formation and on the age of the solutions. By means of TEM, Lloyd and Hair[115b] observed that Pu(IV) forms small (2 nm), spherical PuO_2 colloids of fcc structure. These primary particles agglomerate and form larger entities, which is in good agreement with the behavior of also spherical Th(IV) colloids.[124b,125e,133,140] Small-angle neutron scattering experiments of colloidal Pu(IV) suspensions after a few months of aging revealed the presence of thin rodlike Pu(IV) particles.[161] The morphology change is accompanied by structural transformations and pronounced changes of the chemical properties. Freshly formed colloids dissolve easily upon dilution at constant pH[164,177] or acidification.[124e,157,161] Aging leads to transformation of hydroxide bonds to oxygen bonds (oxolation),[135,178] lowering the solubility,[124f] and are often referred to as "insoluble Pu(IV) polymer".[124g] Very thorough EXAFS studies on many Pu compounds and various solution species[43,125d,179] reveal an astonishing variety of structures and provide clear evidence for elimination of protonated species from freshly formed precipitates during aging and a contribution of higher oxidation states in "Pu(IV) solid phases" aged in contact with oxygen.

4.2.4.4. The Role of Colloids in Pu Redox Chemistry. The presence of higher valent Pu(V) in "Pu(IV) solid phases" is a strong indication that Pu(IV) colloids are in equilibrium with Pu(V) in near neutral solutions[172a] and help understand why some of the redox reactions of Pu (disproportionation of pure Pu(V) solutions) cannot be explained without Pu(IV) colloids as intermediate complexes.[166c] Very recent results show that Pu(IV) colloids and small polymeric species play an important role in thermodynamic Pu equilibrium chemistry,[115c] acting as a link between tri- and tetravalent Pu and the penta- and hexavalent oxo species PuO_2^+ and PuO_2^{2+}.[114]

Costanzo[158a] observed excess reduction of Pu(V) in rather concentrated solutions, which were oversaturated with respect to formation of Pu(IV) hydrous oxide and most likely contained Pu(IV) polymers or colloids. Strong deviations of steady-state distributions were reported[180] over a wide range of acidities and Pu concentrations. Acceleration of the kinetics of redox reactions by Pu(IV) polymers has been suggested,[124d,131a] and Newton et al.[166c] proposed that Pu(V) disproportionation cannot proceed in the absence of Pu(IV) polymers. The importance of the role of Pu polymers and colloids for redox reactions was further corroborated recently.[115c,181] The authors propose, in analogy to the role of the PuO_{2+x} solid[182] (see below), that the formation of mixed valence polymers containing both Pu(IV) and Pu(V) acts as intermediates for redox reactions of Pu(IV) to Pu(V) and vice versa in solution. Haschke[183] postulated the formation of linear or cyclic hydroxo Pu-trimers comprising two Pu(III) and one PuO_2^{2+} ions bridged by hydroxyl groups in disproportionation of Pu(IV) in acidic nitrate and perchlorate solutions. Much earlier but less precise findings pointed in a similar direction to the influence of polymers for disproportionation.[184] One concluding comment concerned PuO_{2+x}, the formation of which was suggested by Haschke[182] and triggered a remarkably large number of theoretical and experimental studies[114,172c,177b,179b,185] (likely due to the claim that water is a reactant in the formation): all samples containing Pu(IV) colloids investigated by EXAFS in the presence of oxygen show a small feature in the FT spectra at ΔR = 1.9 Å. Recently, ref 124g interpreted this in terms of a small contribution of Pu(V), which hints at a PuO_{2+x}-like stoichiometry of the colloids.

4.3. Well-Defined Nanoparticles and Clusters

Whereas nanoparticles in oversaturated solutions are heterogeneous in terms of structure and their size and shape can vary over wide ranges, there are methods of preparing well-characterized monodisperse actinde nanoparticles and nanoclusters. For examples, to prepare uranium nanoparticles, there are hydrothermal methods,[186,187] procedures using porous templates,[188] radiolysis methods with pH control of nanoparticle size and shape,[189] and laser photolysis methods.[190] Starting from soluble species, procedures to generate less soluble species such as electrochemical methods[191,192] can also be used. The amount of literature available for preparation of uranium and thorium particles is vastly greater than for the transuranium elements.

At the University of Notre Dame, Peter Burns and coworkers have a long tradition in synthesizing actinide nanoparticles, summarized, for example, in ref 193 and the contribution to this issue. Recent work includes also attempts to describe their formation using multiconfigurational density functional theory (DFT). Vlaisavljevich et al. analyzed U(VI) ion peroxide nanospheres[194] formation processes on grounds of DFT. Another approach was applied to prove the stability of the large Th(IV) clusters $(Th_{147}O_{292})^{4+}$.[195] A Pu(IV) cluster of high symmetry was reported by Soderholm et al.[82] In that study, well-defined $[Pu_{38}O_{56}Cl_x(H_2O)_y]^{40-x}$ clusters were produced in 0.5 M Pu solution. The starting alkaline peroxide-containing ^{242}Pu solution was acidified with HNO_3 and purified over an anion-exchange resin. This solution contained colloids, and was repeatedly heated, resuspended in HCl, and LiCl added. The clusters were analyzed with high energy X-ray scattering while in solution, but when allowed to evaporate, red crystals form. Surprisingly, their visible light absorption spectra of redissolved red crystals closely resemble that reported by Lloyd and Haire.[115b] This led the authors to hypothesize that these highly symmetric clusters may also form spontaneously in saturated Pu(IV) solutions.

The Burns group has reported a number of nanoscale cage clusters (see refs 196−198 and references therein). These clusters comprise uranyl bipyramid polyhedra, all with uranyl-peroxide-uranyl bridges, some with added linkers that lead to greater potential variations in topologies, cluster size, charges, and pore space size in cluster walls. Hexagon topologies with six edge-sharing uranyl bipyramid polyhedra and generally high symmetry topologies appear to be especially stable.[197] Cage clusters built from uranyl hexagonal bipyramids and oxalate

dx.doi.org/10.1021/cr300343c | Chem. Rev. 2013, 113, 995−1015

(Ox) ligands crystallize from slightly acidic aqueous solution under ambient conditions.[199] It is reported that $U_{50}Ox_{20}$ (with 50 uranyl polyhedra and 20 oxalate molecules) remains intact in aqueous solution upon dissolution of the cage cluster crystals. In the case of $U_{120}Ox_{90}$ clusters with a 2.05 nm radius, made up of an inner $U_{60}Ox_{30}$ cluster inside of a larger cage made up of 12 sets of five edge-sharing uranyl polyhedra (topological pentagons), the $U_{60}Ox_{30}$ core persists in solution. Unruh et al. produced U(VI) nanoscale cage clusters, which self-assemble in alkaline aqueous milieu, some with pyrophosphate linkers.[200] Systematic comparison of the structures reveals that none of the cluster cages contain square−square or square−pentagon adjacencies, whereas square topologies are adjacent to hexagons.

A hexanuclear compound $[M_6\{\mu_3\text{-O (h)}\}_8(HCOO)_{12}(H_2O)_6$ with M = U(IV) and Th(IV)] with a core structure shown in Figure 13 was reported by Takao et al.[201] The structure was

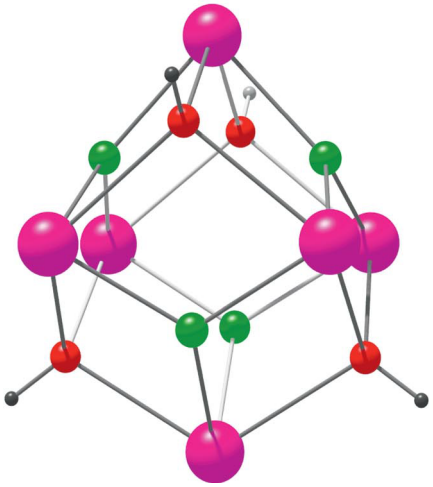

Figure 13. Core structure of $M_6\{\mu_3\text{-O (h)}\}_8(HCOO)_{12}(H_2O)_6$ (pink = Th or U; green = μ_3-O; red = μ_3-OH; black = H). Reproduced with permission from ref 201. Copyright 2009 Wiley-VCH Verlag GmbH & Co. KGaA.

characterized in the solid state by single-crystal X-ray analysis and demonstrated to remain stable in solution using EXAFS spectroscopy. The charge of the hexamer is balanced by the O/OH ratio of the μ_3-bridges. The carboxylic groups (not shown) act as bridges between metal cations, stabilizing the cluster and preventing the formation of larger polynuclear hydrolysis species in solution. Using organic agents to hinder further aggregation and growth of the particles is a strategy often used in synthesis of nanoparticles, including some mentioned at the beginning of this section.[109]

Actinide nanoparticle systems stable in solution described above are particularly interesting for actinide particle research pertaining to environmental issues as models for colloids. Well-defined solid-state systems are also useful models for understanding spectroscopic responses and structure−reactivity relationships. Such solid nanoparticles also have potential applications, as catalysts[187] or as materials for fabrication of nuclear fuels,[189] for example. Krivovichev et al. produced a rich variety of nanostructured solid-state material, including uranyl selenates as summarized recently in ref 202. Particularly remarkable in these uranyl selenate materials is the formation of nanotubules.[203]

Well-defined solid-state hexanuclear clusters for Th(IV), U(IV), Np(IV), and Pu(IV), with 1,2-phenylenediphosphonate as bridging ligand between metal centers, were recently reported.[204,205] They exhibit the formula $M_6(H_2O)_m[C_6H_3(PO_3)(PO_3H)]_6(NO_3)_n)^{6-n}$ (M = Th, U, Np, Pu). The metals are coordinated by five oxygen atoms from the organic ligand and four oxygen atoms from either nitrate anions or water. These clusters exhibit an inner cavity (Figure 14), the size of which is dependent on the ionic radius of the actinide cation (largest for Th(IV) clusters).

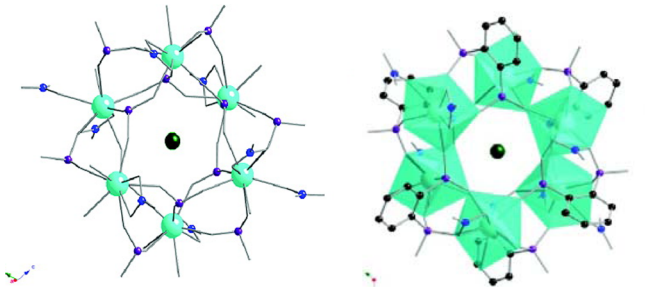

Figure 14. (left) The $Th_6Tl_3[C_6H_4(PO_3)$-$(PO_3H)]_6(NO_3)_7(H_2O)_6\cdot(NO_3)_2(H_2O)_4$ cluster showing the Th_6 core without benzene rings and (right) the Th_6 cluster with Th coordination polyhedra and Tl^+ cation in the inner cavity indicated. Purple = P; blue = N; light green = Th; dark green = Tl. Reprinted with permission from ref 204. Copyright 2012 American Chemical Society.

A recent paper from Wu et al.[206] report the colloidal synthesis of heterodimer nanocrystals of UO_2/In_2O_3 by means of epitaxial growth of In_2O_3 onto UO_2 nanocrystals. Characterization using XRD, EDX, STEM, HRTEM, and structure simulations reveals that epitaxial growth occurs where the affinity for the UO_2 nanocrystals is greatest, as opposed to where lattice mismatch is minimal. In these particles, $(200)UO_2/(400)In_2O_3$ forms the heterojunction (see Figure 15), as at this orientation the indium cations can form three bonds to O atoms at the UO_2 (200) plane. From an environmental relevance point of view, studies such as these can provide insight into the reactivity and stability of actinide

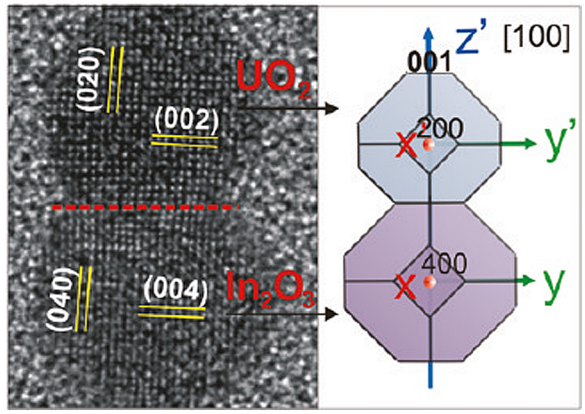

Figure 15. (left) HRTEM image of oa UO_2/In_2O_3 heterodimer nanocrystal. The UO_2 segment is ~5.7 nm and In_2O_3 ~7.7 nm in diameter. Crystal planes are indicated, and the junction between segments is marked with a dotted line. (right) Schematic representation showing the faces. Adapted with permission from ref 206. Copyright 2011 American Chemical Society.

dx.doi.org/10.1021/cr300343c | Chem. Rev. 2013, 113, 995−1015

particles, and aid in predicting hybrid products expected from reactions at particle surfaces, the products of which can potentially serve as model systems for heterogeneous colloids.

5. CONCLUSION AND OUTLOOK

Much of the available literature concerning actinide containing particles of environmental concern does not include rigorous characterization with respect to elemental and isotopic composition, structure, morphology, oxidation state, etc. Missing information in the characterization of such particles can lead to erroneous interpretation and conclusions as to particle origin and potential hazard through transfer to the ecosystem.[207] It remains a challenge of discovery to avoid such errors. The situation is similar in the case of polymers and colloids in solution, where in many cases important chemical information such as pH and redox potential are not or not exactly reported. Calculation of thermodynamic formation constants necessary for predictive assessments is not possible in these cases.

Actinide containing particles exhibit great variability in size, activity, composition, and structure, depending on their source, mode of formation, and history. For example, particles formed from nuclear accidents such as Chenobyl differ strongly from those expected to form in release scenarios from nuclear waste repositories. We have shown above that Chernobyl particles formed in a very high temperature regime from highly crystalline fuel matrix and are found to be rather inert, but do show variations in particle weathering depending on the conditions of release during the accident (explosion versus fire) due to different temperatures, pressures, and oxygen content during these scenarios.[68] Colloids formed in oversaturated solutions such as in a scenario of near surface corrosion of spent nuclear fuel in a waste repository, on the other hand, lead to less well-defined (amorphous) structures, often of An-oxo hydroxo stoichiometry, usually having lower stability. Weathering, oxolation (further condensation), and metamictization can alter these particles, thereby changing properties such as solubility, and hence the risk of leaching, by many orders of magnitude. Such processes can affect the actinide containing particle ecosystem behavior and associated potential human health risks.

It is the potential radiological health risks that were the cause for radioactive particles in general to become a matter of public concern in the 1960s, when the health risk of external exposure (skin contact) and ingestion gave rise to the so-called "hot" particle problem.[1] The actinide elements are both toxic heavy metals and radiotoxic materials. As small nanoparticles, their (radio)toxicity upon human exposure is recognized. Particles of micrometer size and below are easily airborne and inhaled deeply into the human lung. Radioactive particle fallout from nuclear weapons detonations was recognized early on to pose a risk of lung cancer. Alpha emitters of long physical and biological half-life such as plutonium are particularly harmful (1991 ICRP recommendation).[208]

Because of their long-half-lives and persistence in the environment, assessment of health risks of radioactive actinide containing particles in the environment, as well as these particles' stabilities determining their potential hazard will remain subjects of future research. Known variables affecting toxicity of nanoparticles with stable elements (such as quantum dots) include size, charge, concentration, outer coating, bioactivity, and oxidative, photolytic, and mechanical stability.[209] For the most part, these are the same factors we have seen in this discourse to control actinide containing particle stability and mobility in the environment. Surely some of the lessons learned from studies of the toxicity of nanomaterials with stable isotopes can guide research for understanding actinide materials. Along the same train of thought, there is an increasing amount of research material available on the behavior and characteristics of mineral nanoparticles and nanominerals.[210] Lessons learned from studies of their stability, dissolution, and size-related properties can again help steer our research of actinide containing particles. However, these comparisons cannot replace actual studies of actinide containing particles themselves; they can merely provide a comparative platform to help guide research. Actinide particles are α-emitting radioactive systems and the electronic structure and reactivity of the actinide elements are different from the other elements in the periodic system. Although costly, due to the required radiological infrastructure, and very challenging to deal with theoretically (both reasons for the comparative paucity of discoveries in the field), advances in understanding actinide particle formation, reactivity, structure, speciation, and stability, as parameters intimately associated with their weathering, dissolution, mobilization, and being a potential diffuse source of contamination with associated bioavailability, depend on their actual study.

Actinide containing particle research will continue, especially in light of the need to monitor for clandestine nuclear facilities, recent accidents, public awareness, the stringent safety standards of nuclear technologies, and growing global need for low-carbon energy sources. These aspects drive the need to understand actinide chemistry, which is the "backbone of nuclear energy".[211] New advances in instrumentation and available facilities such as free electron lasers will drive future (mass, spatial, energy, temporal) resolution to new limits. Synthesis of synthetic actinide containing particles and studies of their behavior and systematic size-related properties (veritably missing in the literature) with advancing techniques, combined with investigations of anthropogenic and natural particles and support from theoretical progress, will provide process understanding and thermodynamic and kinetic data to reliably predict their hazard potential and to better develop remediation strategies. Time will tell if we one day are able to tailor actinide containing particles according to size and morphologies and thereby discover new materials with interesting properties. To quote from ref 212, "Whereas nanoscience is a very active field when one considers stable elements, it is still in its infancy when dealing with radioactive actinides."

AUTHOR INFORMATION

Corresponding Author

*E-mail: walther@irs.uni-hannover.de.

Notes

The authors declare no competing financial interest.

Biography



Melissa Anne Denecke (left) completed her undergraduate studies at Carroll College, Waukesha, WI and University of Wisconsin–Madison. After completing her graduate studies, culminating in receiving her Doctor rerum naturalium magna cum laude in Physical Chemistry from the University of Hamburg in 1994, she spent a 3 year term in a postdoctoral position at the Research Center Rossendorf, Dresden, Germany. Since 1998, she works at Karlsruhe Institute of Technology (KIT; formerly the Research Center Karlsruhe), Institute for Nuclear Waste Disposal. Initially group leader for "Synchrotron Applications", responsible for the INE-Beamline for Actinide Research at the synchrotron source ANKA, she is presently department head for "Actinide Speciation". Her research interests include f-element chemistry, X-ray spectroscopy, instrumental method development, separations of lanthanide and actinide elements, natural analogue investigations, and other aspects of the nuclear fuel cycle. She is the proud mother of two (now grown) children.

Clemens Walther (right) studied physics at the University of Mainz, obtaining his Ph.D. from the Institute for Nuclear Chemistry in 1998, under the supervision of Professor Dr. J. V. Kratz. During this time, he spent a research year at the University of Washington (Seattle) in the group of Professor Fordson. He completed his habilitation, "Venia legendi", in Nuclear Chemistry in Mainz in 2008, where he also served as lecturer in 2008. From 1999 to 2011, he was employed at the Research Center Karlsruhe, later Karlsruhe Institute of Technology, in the Institute for Nuclear Waste Disposal, serving as group leader "Nanoparticle Analysis" and deputy department head of "Actinide Speciation". He is currently professor and head of the Institute for Radioecology and Radiation Protection at the Leibniz University Hannover.

REFERENCES

(1) Charles, M. W.; Harrison, J. D. *J. Radiol. Prot.* **2007**, *27*, A97.
(2) UNSCEAR. *Sources and Effects of Ionizing Radiation*; United Nations Scientific Committee on the Effects of Atomic Radiation, 2010.
(3) Edvarson, K.; Low, K.; Sisefsky, J. *Nature* **1959**, *184*, 1771.
(4) Freiling, E. C. *Science* **1961**, *133*, 1991.
(5) IAEA. *Radioactive Particles in the Environment: Sources, Particle Characterization and Analytical Techniques*; International International Atomic Energy Agency TECDOC 1663, 2011.
(6) Lind, O. C.; Nygren, U.; Thaning, L.; Ramebäck, H.; Sidhu, R. S.; Roos, P.; Pöllänen, R.; Ranebo, Y.; Holm, E.; Salbu, B. Overview of sources of radioactive particles of Nordic relevance as well as a short description of available particle characterisation techniques. *NKS HOT II Report*, 2008.
(7) Flegler, S. L.; Heckman, J. W.; Klomparens, K. L. *Scanning and Transmission Electron Microscopy*; Oxford University Press: Oxford, 1993.
(8) Hornyaka, G. L.; Peschela, S.; Sawitowskia, T.; Schmid, G. *Micron* **1998**, *29*, 183.
(9) Gross, J. H. *Mass Spectrometry*; Springer: Berlin, 2004.
(10) (a) Becker, J. S. *Spectrochim. Acta, Part B* **2003**, *58*, 1757. (b) Ketterer, M. E.; Szechenyi, S. C. *Spectrochim. Acta, Part B* **2008**, *63*, 719.
(11) Fifield, L. K.; Cresswell, R. G.; Tada, M. L. d.; T, R. O.; Day, J. P.; Clacher, A. P.; King, S. J.; Priest, N. D. *Nucl. Instrum. Methods Phys. Res., Sect. B* **1996**, *117*, 295.
(12) De Laeter, J. R. *Applications of Inorganic Mass Spectrometry*; John Wiley & Sons: New York, 2001.
(13) Di Marco, V. B.; Bombi, G. G. *Mass Spectrom. Rev.* **2006**, *25*, 347.
(14) Soto-Guerrero, J.; Gajdosova, D.; Havel, J. *J. Radioanal. Nucl. Chem.* **2001**, *249*, 139.
(15) Trautmann, N.; Passler, G.; Wendt, K. D. A. *Anal. Bioanal. Chem.* **2004**, *378*, 348.
(16) Rothe, J.; Walther, C.; Brendebach, B.; Buchner, S.; Fuss, M.; Denecke, M. A.; Geckeis, H. *14th International Conference on X-Ray Absorption Fine Structure (Xafs14), Proceedings*, 2009; Vol. *190*.
(17) *Actinide Nanoparticle Research*; Springer Verlag: Heidelberg, 2011.
(18) Landa, E. R.; Stieff, L. R.; Germani, M. S.; Tanner, A. B.; Evans, J. R. *Nucl. Geophys.* **1994**, *8*, 443.
(19) Deditius, A. P.; Pointeau, V.; Zhang, J. M.; Ewing, R. C. *Am. Mineral.* **2012**, *97*, 681.
(20) Deditius, A. P.; Utsunomiya, S.; Pointeau, V.; Ewing, R. C. *Eur. J. Mineral.* **2010**, *22*, 75.
(21) Deditius, A. P.; Utsunomiya, S.; Ewing, R. C. *Chem. Geol.* **2008**, *251*, 33.
(22) Finch, R.; Murakami, T. *Rev. Mineral.* **1999**, *38*, 91.
(23) Murakami, T.; Ohnuki, T.; Isobe, H.; Sato, T. *Am. Mineral.* **1997**, *82*, 888.
(24) Woodhead, J. A.; Rossman, G. E. *Am. Mineral.* **1991**, *76*, 74.
(25) Salje, E. K. H.; Chrosch, J.; Ewing, R. C. *Am. Mineral.* **1999**, *84*, 1107.
(26) Tromans, D. *J. Nucl. Mater.* **2006**, *357*, 221.
(27) Balan, E.; Neuville, D. R.; Trocellier, P.; Fritsch, E.; Muller, J.-P.; Calas, G. *Am. Mineral.* **2001**, *89*, 1025.
(28) Utsunomiya, S.; Jensen, K. A.; Keeler, G. J.; Ewing, R. C. *Environ. Sci. Technol.* **2002**, *36*, 4943.
(29) Utsunomiya, S.; Kogawa, M.; Kamiishi, E.; Ewing, R. C. In *Actinide Nanoparticle Research*; Kalmykov, S. N., Denecke, M. A., Eds.; Springer: Heidelberg, 2011.
(30) Lovley, D. R.; Phillips, E. J. P.; Gorby, Y. A.; Landa, E. R. *Nature* **1991**, *350*, 413.
(31) Merroun, M. L.; Selenska-Pobell, S. *J. Contam. Hydrol.* **2008**, *102*, 285.
(32) Fayek, M.; Utsunomiya, S.; Pfiffner, S. M.; White, D. C.; Riciputi, L. R.; Ewing, R. C.; Anovitz, L. M.; Stadermann, F. J. *Can. Mineral.* **2005**, *43*, 1631.
(33) Lloyd, J. R. *FEMS Microbiol. Rev.* **2003**, *27*, 411.
(34) Lloyd, J. R.; Chesnes, J.; Glasauer, S.; Bunker, D. J.; Livens, F. R.; Lovley, D. R. *Geomicrobiol. J.* **2002**, *19*, 103.
(35) Barlett, M.; Moon, H. S.; Peacock, A. A.; Hedrick, D. B.; Williams, K. H.; Long, P. E.; Lovley, D.; Jaffe, P. R. *Biodegradation* **2012**, *23*, 535.
(36) Bargar, J. R.; Bernier-Latmani, R.; Giammar, D. E.; Tebo, B. M. *Elements* **2008**, *4*, 407.
(37) Schofield, E. J.; Veeramani, H.; Sharp, J. O.; Suvorova, E.; Bernier-Latmani, R.; Mehta, A.; Stahlman, J.; Webb, S. M.; Clark, D. L.; Conradson, S. D.; Ilton, E. S.; Bargar, J. R. *Environ. Sci. Technol.* **2008**, *42*, 7898.

(38) Ulrich, K. U.; Singh, A.; Schofield, E. J.; Bargar, J. R.; Veeramani, H.; Sharp, J. O.; Bernier-Latmani, R.; Giammar, D. E. *Environ. Sci. Technol.* **2008**, *42*, 5600.
(39) Ulrich, K. U.; Ilton, E. S.; Veeramani, H.; Sharp, J. O.; Bernier-Latmani, R.; Schofield, E. J.; Bargar, J. R.; Giammar, D. E. *Geochim. Cosmochim. Acta* **2009**, *73*, 6065.
(40) Grossmann, K.; Arnold, T.; Krawczyk-Barsch, E.; Diessner, S.; Wobus, A.; Bernhard, G.; Krawietz, R. *Environ. Sci. Technol.* **2007**, *41*, 6498.
(41) Neu, M. P.; Icopini, G. A.; Boukhalfa, H. *Radiochim. Acta* **2005**, *93*, 705.
(42) Jensen, M. P.; Aryal, B. P.; Gorman-Lewis, D.; Paunesku, T.; Lai, B.; Vogt, S.; Woloschak, G. E. *Anal. Chim. Acta* **2012**, *722*, 21.
(43) Rothe, J.; Walther, C.; Denecke, M. A.; Fanghänel, T. *Inorg. Chem.* **2004**, *43*, 4708.
(44) Laeter, J. R. d. *Applications of Inorganic Mass Spectrometry*; Wiley-Interscience: New York, 2001.
(45) Veryovkin, I. V. C.; Wallis, F.; Moore, J. F.; Pellin, M. J.; Burnett, D. S. *Nucl. Instrum. Methods Phys. Res., Sect. B* **2004**, 473.
(46) Salbu, B. *Integr. Environ. Assess. Manage.* **2011**, *7*, 362.
(47) Lind, O. C.; Salbu, B.; Janssens, K.; Proost, K.; Danesi, P. R. In *Radioactive Particles in the Environment*; Oughton, D. H. K. V., Ed.; Springer: New York, 2009.
(48) Moulin, V.; Moulin, C. *Radiochim. Acta* **2001**, *89*, 773.
(49) Luo, M.; Hu, B.; Zhang, X.; Peng, D.; Chen, H.; Zhang, L.; Huan, Y. *Anal. Chem.* **2010**, *82*, 282.
(50) (a) Jernström, J.; Eriksson, M.; Simon, R.; Tamborini, G.; Bildstein, O.; Marquez, R. C.; Kehl, S. R.; Hamilton, T. F.; Ranebo, Y.; Betti, M. *Spectrochim. Acta, Part B* **2006**, *61*, 971. (b) Lind, O. C.; Salbu, B.; Janssens, K.; Proost, K.; Garcia-Leon, M.; Garcia-Tenorio, R. *Sci. Total Environ.* **2007**, *376*, 294. (c) Raynal, P. I.; Quirico, E.; Borg, J.; Deboffle, D.; Dumas, P.; d'Hendecourt, L.; Bibring, J. P.; Langevin, Y. *Planet. Space Sci.* **2000**, *48*, 1329. (d) Osán, J.; Török, S.; Alföldy, B.; Falkenberg, G. *Spectrochim. Acta, Part B* **2004**, *59*, 701. (e) Patel, M.; Azanza Ricardo, C. L.; Scardi, P.; Aswath, P. B. *Tribol. Int.* **2012**, *52*, 29. (f) Baruchel, J.; Buffiere, J.-Y.; Cloetens, P.; Di Michiel, M.; Ferrie, E.; Ludwig, W.; Maire, E.; Salvo, L. *Scr. Mater.* **2006**, *55*, 41. (g) Zbik, M. S.; Frost, R. L.; Song, Y.-F. *J. Colloid Interface Sci.* **2008**, *319*, 169. (h) Bukowiecki, N.; Lienemann, P.; Zwicky, C. N.; Furger, M.; Richard, A.; Falkenberg, G.; Rickers, K.; Grolimund, D.; Borca, C.; Hill, M.; Gehrig, R.; Baltensperger, U. *Spectrochim. Acta, Part B* **2008**, *63*, 929. (i) Borg, J.; Djouadi, Z.; Grossemy, F.; Eichert, D.; Martinez-Criado, G.; Westphal, A. J.; Deboffle, D.; Snead, C. J.; Somogyi, A. *Adv. Space Res.* **2006**, *38*, 2068.
(51) Torok, S.; Osan, J.; Vincze, L.; Alfoldy, B.; Kerkapoly, A.; Vajda, N.; Perez, C. A.; Falkenberg, G. *J. Anal. At. Spectrom.* **2003**, *18*, 1202.
(52) Erdmann, N.; Kratz, J. V.; Trautmann, N.; Passler, G. *Anal. Bioanal. Chem.* **2009**, *395*, 1911.
(53) Eriksson, M.; Osan, J.; Jernstrom, J.; Wegrzynek, D.; Simon, R.; Chinea-Cano, E.; Markowicz, A.; Bamford, S.; Tamborini, G.; Torok, S.; Falkenberg, G.; Alsecz, A.; Dahlgaard, H.; Wobrauschek, P.; Streli, C.; Zoeger, N.; Betti, M. *Spectrochim. Acta, Part B* **2005**, *60*, 455.
(54) Shinonaga, T.; Esaka, F.; Magara, M.; Klose, D.; Donohue, D. *Spectrochim. Acta, Part B* **2008**, *63*, 1324.
(55) Esaka, F.; Esaka, K. T.; Lee, C. G.; Magara, M.; Sakurai, S.; Usuda, S.; Watanabe, K. *Talanta* **2007**, *71*, 1011.
(56) Hamilton, T. F.; Jernstroeem, J.; Martinelli, R. E.; Kehl, S. R.; Eriksson, M.; Williams, R. W.; Bielewski, M.; Rivers, A. N.; Brown, T. A.; Tumey, S. J.; Betti, M. *J. Radioanal. Nucl. Chem.* **2009**, *282*, 1019.
(57) Danesi, P. R.; Markowicz, A.; Chinea-Cano, E.; Burkart, W.; Salbu, B.; Donohue, D.; Ruedenauer, F.; Hedberg, M.; Vogt, S.; Zahradnik, P.; Ciurapinski, A. *J. Environ. Rad.* **2003**, *64*, 143.
(58) Report "Depleted Uranium in Kosovo Post-Conflict Environmental Assessment", United Nations Environment Programme, 2001.
(59) Bürger, S.; Buda, R. A.; Geckeis, H.; Huber, G.; Kratz, J. V.; Kunz, P.; Gostomski, C. L. v.; Passler, G.; Remmert, A.; Trautmann, N. In *Radioactivity in the Environment*; Povinec, P. P., Sanchez-Cabeza, J. A., Eds.; NEA/OECD, 2006; Vol. *8*.
(60) Entwistle, J. A.; Flowers, A. G.; Nageldinger, G.; Greenwood, J. C. *Mineral. Mag.* **2003**, *67*, 183.
(61) Salbu, B.; Krekling, T.; Lind, O. C.; Oughton, D. H.; Drakopoulos, M.; Simionovici, A.; Snigireva, I.; Snigirev, A.; Weitkamp, T.; Adams, F.; Janssens, K.; Kashparov, V. A. *Nucl. Instrum. Methods* **2001**, *467*, 1249.
(62) (a) Kashparov, V.; Ahamdach, N.; Levchuk, S.; Yoschenko, V.; Fesenko, S.; Maloshtan, I. In *Radioactive Particles in the Environment*; Oughton, D. H., Kashparov, V., Eds.; Springer: New York, 2009. (b) Kashparov, V.; Yoschenko, V.; Levchuk, S.; Bugai, D.; Van Meir, N.; Simonucci, C.; Martin-Garin, A. *Appl. Geochem.* **2012**, *27*, 1348.
(63) Burns, P. C.; Ewing, R. C.; Navrotsky, A. *Science* **2012**, *335*, 1184.
(64) Levchuk, S.; Kashparov, V.; Maloshtan, I.; Yoschenko, V.; Van Meir, N. *Appl. Geochem.* **2012**, *27*, 1339.
(65) Hamilton, E. I. *Mineral. Mag.* **1985**, *49*, 177.
(66) (a) Kershaw, P. J.; McCubbin, D.; Leonard, K. S. *Sci. Total Environ.* **1999**, *238*, 119. (b) Kershaw, P. J.; Denoon, D. C.; Woodhead, D. S. *J. Environ. Radioact.* **1999**, *44*, 191.
(67) Dennis, F.; Morgan, G.; Henderson, F. *J. Radiol. Prot.* **2007**, *27*, A3.
(68) Salbu, B. In *Radioactive Particles in the Environment*; Oughton, D. H., Kashparov, V., Eds.; Springer: New York, 2009.
(69) Salbu, B. *J. Environ. Radioact.* **2007**, *96*, 47.
(70) Salbu, B.; Nikitin, A. I.; Strand, P.; Christensen, G. C.; Chumichev, V. B.; Lind, B.; Fjelldal, H.; Bergan, T. D. S.; Rudjord, A. L.; Sickel, M.; Valetova, N. K.; Foyn, L. *Sci. Total Environ.* **1997**, *202*, 185.
(71) Kjerre, L. Ph.D. Thesis, Nowegian University of Life Sciences, 2006.
(72) Litaor, M. I.; Barth, G. R.; Zika, E. M. *Environ. Qual.* **1996**, *25*, 671.
(73) Stubbs, J. E.; Veblen, L. A.; Elbert, D. C.; Zachara, J. M.; Davis, J. A.; Veblen, D. R. *Geochim. Cosmochim. Acta* **2009**, *73*, 1563.
(74) Giere, R.; Kaltenmeier, R.; Pourcelot, L. *J. Environ. Monit.* **2012**, *14*, 1264.
(75) Nair, S. K.; Chambers, D. B.; Radonjic, Z.; Park, S. *Atmos. Environ.* **1998**, *32*, 1729.
(76) Guimbretiere, G.; Canizares, A.; Simon, P.; Tobon-Correa, Y. A.; Ammar, M. R.; Corbel, C.; Barthe, M. F. *Spectrosc. Lett.* **2011**, *44*, 570.
(77) Shoesmith, D. W. *J. Nucl. Mater.* **2000**, *282*, 1.
(78) Amme, M.; Renker, B.; Schmid, B.; Feth, M. P.; Bertagnolli, H.; Döbelin, W. *J. Nucl. Mater.* **2002**, *306*, 202.
(79) Clarens, F.; De Pablo, J.; DÃez-Perez, I.; Casas, I.; Gimenez, J.; Rovira, M. *Environ. Sci. Technol.* **2004**, *38*, 6656.
(80) Arnold, T.; Utsunomiya, S.; Geipel, G.; Ewing, R. C.; Baumann, N.; Brendler, V. *Environ. Sci. Technol.* **2006**, *40*, 4646.
(81) Schmidt, M.; Wilson, R. E.; Lee, S. S.; Soderholm, L.; Fenter, P. *Langmuir* **2012**, *28*, 2620.
(82) Soderholm, L.; Almond, P. M.; Skanthakumar, S.; Wilson, R. E.; Burns, P. C. *Angew. Chem., Int. Ed.* **2008**, *47*, 298.
(83) Ewing, R. C.; Runde, W.; Albrecht-Schmitt, T. E. *MRS Bull.* **2010**, *35*, 859.
(84) Kretzschmar, R.; Barmettler, K.; Grolimund, D.; Yan, Y.-d.; Borkovec, M.; Sticher, H. *Water Resour. Res.* **1997**, *33*, 1129.
(85) Geckeis, H.; Schäfer, T.; Hauser, W.; Rabung, T.; Missana, T.; Degueldre, C.; Möri, A.; Eikenberg, J.; Fierz, T.; Alexander, W. R. *Radiochim. Acta* **2004**, *92*, 765.
(86) Kersting, A. B.; Efurd, D. W.; Finnegan, D. L.; Rokop, D. J.; Smith, D. K.; Thompson, J. L. *Nature* **1999**, *397*, 56.
(87) Utsunomiya, S.; Kersting, A. B.; Ewing, R. C. *Environ. Sci. Technol.* **2009**, *43*, 1293.
(88) Novikov, A. P.; Kalmykov, S. N.; Utsunomiya, S.; Ewing, R. C.; Horreard, F.; Merkulov, A.; Clark, S. B.; Tkachev, V. V.; Myasoedov, B. F. *Science* **2006**, *314*, 638.
(89) Dai, M.; Kelley, J. M.; Buesseler, K. O. *Environ. Sci. Technol.* **2002**, *36*, 3690.

(90) Donard, O. F. X.; Bruneau, F.; Moldovan, M.; Garraud, H.; Epov, V. N.; Boust, D. *Anal. Chim. Acta* **2007**, *587*, 170.
(91) Zheng, J.; Yamada, M. *Environ. Sci. Technol.* **2006**, *40*, 4103.
(92) Pentreath, R. J. *Cont. Shelf Res.* **1987**, *7*, 1457.
(93) Buck, E. C.; Bates, J. K. *Appl. Geochem.* **1999**, *14*, 635.
(94) Kim, J. I.; Treiber, W.; Lierse, C.; Offermann, P. *Scientific Basis for Nuclear Waste Management VIII*; Boston, MA, 1984; p 359.
(95) Geckeis, H. *Geological Society Special Publication*, 2004.
(96) Xie, J.; Lu, J.; Zhou, X.; Wang, X.; Li, M.; Du, L.; Zhou, G. *Chemosphere* **2012**, *87*, 925.
(97) Francis, A. J.; Dodge, C. J.; Gillow, J. B. *Radiochim. Acta* **2006**, *94*, 731.
(98) Stetzer, O.; Betti, M.; van Geel, J.; Erdmann, N.; Kratz, J. V.; Schenkel, R.; Trautmann, N. *Nucl. Instrum. Methods* **2004**, *525*, 582.
(99) Shen, Y.; Zhao, Y. G.; Guo, S. L.; Cui, J. Y.; Liu, Y.; Li, J. H.; Xu, J.; Zhang, H. Z. *Radiat. Meas.* **2008**, *43*, S299.
(100) Esaka, F.; Watanabe, K.; Onodera, T.; Lee, C. G.; Magara, M.; Sakurai, S.; Usuda, S. *Appl. Surf. Sci.* **2008**, *255*, 1512.
(101) Zhang, X. Z.; Esaka, F.; Esaka, K. T.; Magara, M.; Sakurai, S.; Usuda, S.; Watanabe, K. *Spectrochim. Acta, Part B* **2007**, *62*, 1130.
(102) Wallenius, M.; Tamborini, G.; Koch, L. *Radiochim. Acta* **2001**, *89*, 55.
(103) Ranebo, Y.; Hedberg, P. M. L.; Whitehouse, M. J.; Ingeneri, K.; Littmann, S. *J. Anal. At. Spectrom.* **2009**, *24*, 277.
(104) Kips, R. S.; Kristo, M. J. *J. Radioanal. Nucl. Chem.* **2009**, *282*, 1031.
(105) Ranebo, Y.; Niagolova, N.; Erdmann, N.; Eriksson, M.; Tamborini, G.; Betti, M. *Anal. Chem.* **2010**, *82*, 4055.
(106) Varga, Z. *Anal. Chim. Acta* **2008**, *625*, 1.
(107) Erdmann, N.; Betti, M.; Stetzer, O.; Tamborini, G.; Kratz, J. V.; Trautmann, N.; van Geel, J. *Spectrochim. Acta, Part B* **2000**, *55*, 1565.
(108) Erdmann "Internal Report", JRC ITU.
(109) Hudry, D.; Apostolidis, C.; Walter, O.; Gouder, T.; Courtois, E.; Kübel, C.; Meyer, D. *Chem.-Eur. J.* **2012**, *18*, 8283.
(110) Lünsdorf, H.; Kristen, I.; Barth, E. *BMC Microbiol.* **2006**, *6*.
(111) Shinonaga, T.; Donohue, D.; Aigner, H.; Bürger, S.; Klose, D.; Kärkelä, T.; Zilliacus, R.; Auvinen, A.; Marie, O.; Pointurier, F. *Anal. Chem.* **2011**, *84*, 2638.
(112) Schindler, P. W. *Adv. Chem. Ser.* **1967**, *67*, 196.
(113) (a) Bundschuh, T.; Knopp, R.; Müller, R.; Kim, J. I.; Neck, V.; Fanghänel, T. *Radiochim. Acta* **2000**, *88*, 625. (b) Neck, V.; Altmaier, M.; Müller, R.; Bauer, A.; Fanghänel, T.; Kim, J. I. *Radiochim. Acta* **2003**, *91*, 253. (c) Fanghänel, T.; Neck, V. *Pure Appl. Chem.* **2002**, *74*, 1895.
(114) Neck, V.; Altmaier, M.; Seibert, A.; Yun, J. I.; Marquardt, C. M.; Fanghänel, T. *Radiochim. Acta* **2007**, *95*, 193.
(115) (a) Walther, C.; Cho, H. R.; Marquardt, C. M.; Neck, V.; Seibert, A.; Yun, J. I.; Fanghänel, T. *Radiochim. Acta* **2007**, *95*, 7. (b) Lloyd, M. H.; Haire, R. G. *Radiochim. Acta* **1978**, *25*, 139. (c) Walther, C.; Rothe, J.; Brendebach, B.; Fuss, M.; Altmaier, M.; Marquardt, C. M.; Büchner, S.; Cho, H.-R.; Yun, J.-I. *Radiochim. Acta* **2009**, *97*, 199. (d) Wilson, R. E.; Hu, Y. J.; Nitsche, H. *Radiochim. Acta* **2005**, *93*, 203.
(116) Borkovec, M. In *Handbook of Applied Surface and Colloid Chemistry*; Holmberg, K., Ed.; John Wiley and Sons: New York, 2002; Vol. *2*.
(117) (a) Kitamori, T.; Matsui, T.; Sakagami, M. *Chem. Lett.* **1989**, *89*, 2205. (b) Kim, J. I.; Walther, C. In *Environmental Colloids and Particles: Behaviour, Separation and Characterisation*; Lead, J., Wilkinson, K., Eds.; John Wiley & Sons: West Sussex, 2007; Vol. *10*. (c) Walther, C.; Büchner, S.; Filella, M.; Chanudet, V. *J. Colloid Interface Sci.* **2006**, *301*, 532.
(118) Cole, R. B. *Electrospray Ionization Mass Spectrometry*; John Wiley and Sons: New York, 1997.
(119) Keith-Roach, M. J.; Buratti, M. V.; Worsfold, P. J. *Anal. Chem.* **2005**, *77*, 7335.
(120) Degueldre, C.; Favarger, P. Y. *Talanta* **2004**, *62*, 1051.
(121) Degueldre, C.; Favarger, P. Y.; Rosse, R.; Wold, S. *Talanta* **2006**, *68*, 623.
(122) Metivier, H.; Guillaumont, R. *Radiochem. Radioanal. Lett.* **1972**, *10*, 27.
(123) Runde, W. *Los Alamos Sci.* **2000**, *26*, 392.
(124) (a) Rabideau, S. W. *J. Am. Chem. Soc.* **1953**, *75*, 798. (b) Kraus, K. A. *International Conference on the Peaceful Use of Atomic Energy*; Geneva, Switzerland, 1956; p 245. (c) Choppin, G. R. *Radiochim. Acta* **1983**, *32*, 43. (d) Newton, T. W.; Rundberg, V. L. *Materials Research Society Annual Meeting*; Boston, MA, 1983; p 867. (e) Cleveland, J. M. *The Chemistry of Plutonium*, 2nd ed.; American Nuclear Society: La Grange Park, IL, 1979. (f) Zhao, P.; Steward, S. A. *LLNL Report* **1997**, *126039*, 2. (g) Clark, D. L.; Hecker, S. S.; Jarvinen, G. D.; Neu, M. P. In *The Chemistry of Actinide and Transactinide Elements*, 3rd ed.; Morss, L. R., Edelstein, N. M., Fuger, J., Katz, J. J., Eds.; Springer: New York, 2006; Vol. *2*.
(125) (a) Neck, V.; Müller, R.; Bouby, M.; Altmaier, M.; Rothe, J.; Denecke, M. A.; Kim, J. I. *Radiochim. Acta* **2002**, *90*, 485. (b) Bitea, C.; Müller, R.; Neck, V.; Walther, C.; Kim, J. I. *Colloids Surf., A* **2003**, *217*, 63. (c) Walther, C.; Fuss, M.; Büchner, S.; Geckeis, H. *J. Radioanal. Nucl. Chem.* **2009**, *282*, 1003. (d) Rothe, J.; Walther, C.; Brendebach, B.; Büchner, S.; Fuss, M.; Denecke, M. A.; Geckeis, H. *J. Phys. Conf. Ser.* **2009**, *190*, 012188. (e) Walther, C. *Colloids Surf., A* **2003**, *217*, 81.
(126) Knopp, R.; Neck, V.; Kim, J. I. *Radiochim. Acta* **1999**, *86*, 101.
(127) (a) Guillaumont, R.; Fanghänel, T.; Fuger, J.; Grenthe, I.; Neck, V.; Palmer, D. A.; Rand, M. H. *Update on the Chemical Thermodynamics of Uranium, Neptunium, Plutonium, Americium and Technecium*; Elsevier, North-Holland: Amsterdam, 2003. (b) Opel, K.; Weiß, S.; Hübener, S.; Zänker, H.; Bernhard, G. *Radiochim. Acta* **2007**, *95*, 143.
(128) Neck, V.; Kim, J. I.; Seidel, B. S.; Marquardt, C. M.; Dardenne, K.; Jensen, M. P.; Hauser, W. *Radiochim. Acta* **2001**, *89*, 439.
(129) (a) Marquardt, C. M.; Panak, P. J.; Apostolidis, C.; Morgenstern, A.; Walther, C.; Klenze, R.; Fanghänel, T. *Radiochim. Acta* **2004**, *92*, 445. (b) Marquardt, C. M.; Panak, P. J.; Walther, C.; Klenze, R.; Fanghänel, T. *Recent Advances in Actinide Science*; Royal Society of Chemistry: Manchester, 2005; p 776. (c) Tarapcik, P.; Fourest, B.; Giffaut, E. *Radiochim. Acta* **2005**, *93*, 27. (d) Myasoedov, B. F.; Kirby, H. W.; Tananaev, I. G. In *The Chemistry of Actinide and Transactinide Elements*, 3rd ed.; Morss, L. R., Edelstein, N. M., Fuger, J., Katz, J. J., Eds.; Springer: New York, 2006; Vol. *1*.
(130) (a) Moulin, C.; Charron, N.; Plancque, G.; Virelizier, H. *Appl. Spectrosc.* **2000**, *54*, 843. (b) Moulin, C. *Radiochim. Acta* **2003**, *91*, 651. (c) Steppert, M.; Walther, C.; Fuss, M.; Büchner, S. *Rapid Commun. Mass Spectrom.* **2012**, *26*, 583. (d) Jung, E. C.; Cho, H. R.; Park, K. K.; Yeon, J. W.; Song, K. *Appl. Phys. B: Laser Opt.* **2009**, *97*, 867.
(131) (a) Madic, C.; Begun, G. M.; Hobart, D. E.; Hahn, R. L. *Inorg. Chem.* **1984**, *23*, 1914. (b) Gaunt, A.; May, I.; Neu, M. P.; Reilly, S. D.; Scott, B. L. *Inorg. Chem.* **2011**, *50*, 4244. (c) Cassol, A.; Magnon, L.; Portanova, R.; Tondello, E. *Radiochim. Acta* **1972**, *17*, 28. (d) Reilly, S. D.; Neu, M. P. *Inorg. Chem.* **2006**, *45*, 1839. (e) Cho, H. R.; Jung, E. C.; Park, K. K.; Song, K.; Yun, J. I. *Radiochim. Acta* **2010**, *98*, 555.
(132) Steppert, M.; Walther, C. *Radiochim. Acta.* **2012**, in print.
(133) Wickleder, M.; Fourest, B.; Dorhout, P. In *The Chemistry of Actinide and Transactinide Elements*, 3rd ed.; Morss, L. R., Edelstein, N. M., Fuger, J., Katz, J. J., Eds.; Springer: New York, 2006; Vol. *1*.
(134) Rand, M. H.; Fuger, J.; Grenthe, I.; Neck, V.; Rai, D. *Chemical Thermodynamics of Thorium*; Elsevier, North-Holland: Amsterdam, 2009.
(135) Johnson, G. L.; Toth, L. M. *Plutonium(IV) and Thorium(IV) Hydrous Polymer Chemistry*; Oak Ridge National Laboratory: Oak Ridge, TN, 1978.
(136) Neck, V.; Kim, J. I. *Radiochim. Acta* **2001**, *89*, 1.
(137) Choppin, G. R.; Rizkalla, E. N. In *Handbook on the Physics and Chemistry of Rare Earths*; Gschneider, K. A., Jr., Eyring, L., Choppin, G. R., Lander, G. H., Eds.; North Holland Elsevier Science Publishers B.V.: Amsterdam, The Netherlands, 1994; Vol. *18*.
(138) Moll, H.; Denecke, M. A.; Jalilehvand, F.; Sandström, M.; Grenthe, I. *Inorg. Chem.* **1999**, *38*, 1795.
(139) Rothe, J.; Denecke, M. A.; Neck, V.; Müller, R.; Kim, J. I. *Inorg. Chem.* **2002**, *41*, 249.

(140) Dzimitrowicz, D. J.; Wiseman, P. J.; Cherns, D. *J. Colloid Interface Sci.* **1985**, *103*, 170.
(141) Katz, J. J. *Chemistry of the Actinide Elements*; Chapman and Hall: London, 1986.
(142) (a) Sillen, L. G. *Symposium on Coordination Chemistry*; Copenhagen, 1953; p 74. (b) Kim, J. I. *Mater. Res. Soc. Bull.* **1994**, *19*, 47.
(143) Yoshida, Z.; Johnson, S. G.; Kimura, T.; Krsul, J. R. In *The Chemistry of Actinide and Transactinide Elements*; Morss, L. R., Edelstein, N. M., Fuger, J., Katz, J. J., Eds.; Springer: Heidelberg, 2006; Vol. *2*.
(144) (a) Stumpe, R.; Kim, J. I.; Schrepp, W.; Walther, H. *Appl. Phys. B: Laser Opt.* **1984**, *34*, 203. (b) Klenze, R.; Kim, J. I.; Wimmer, H. *Radiochim. Acta* **1991**, *52*−*3*, 97.
(145) Denecke, M. A.; Nolf, W. d.; Rack, A.; Tucoulou, R.; Vitova, T.; Falkenberg, G.; Abolhassani, S.; Cloetens, P.; Kienzler, B. In *Actinide Nanoparticle Research*; Kalmykov, S. N., Denecke, M. A., Eds.; Springer Verlag: Heidleberg, 2011.
(146) Denecke, M. A.; Brendebach, B.; Nolf, W. D.; Falkenberg, G.; Janssens, K.; Simon, R. *Spectrochim. Acta, Part B* **2009**, *64*, 791.
(147) Krot, N. N.; Grigoriev, M. S. *Russ. Chem. Rev.* **2004**, *73*, 94.
(148) (a) Nocton, G.; Horeglad, P.; Pecaut, J.; Mazzanti, M. *J. Am. Chem. Soc.* **2008**, *130*, 16633. (b) Forbes, T. Z.; Burns, P. C. *J. Solid State Chem.* **2009**, *182*, 43. (c) Natrajan, L.; Burdet, F.; Pecaut, J.; Mazzanti, M. *J. Am. Chem. Soc.* **2006**, *128*, 7152.
(149) Mougel, V.; Horeglad, P.; Nocton, G.; Pecaut, J.; Mazzanti, M. *Chem.-Eur. J.* **2010**, *16*, 14365.
(150) Grenthe, I.; Drozdzynski, J.; Fujino, T.; Buck, E. C.; Albrecht-Schmitt, T. E.; Wolf, S. E. *Uranium*; Springer: Dodrecht, Netherlands, 2008.
(151) Cho, H.-R.; Jung, E. C.; Jee, K. Y. *Jpn. J. Appl. Phys.* **2008**, *47*, 3530.
(152) Somogyi, A.; Pasilis, S. P.; Pemberton, J. E. *Int. J. Mass Spectrom.* **2007**, *265*, 281.
(153) Moulin, C.; Amekraz, B.; Colette, S.; Doizi, D.; Jacopin, C.; Lamouroux, C.; Plancque, G. *J. Alloys Compd.* **2006**, *408*, 1242.
(154) Tsierkezos, N. G.; Roithova, J.; Schroder, D.; Oncak, M.; Slavicek, P. *Inorg. Chem.* **2009**, *48*, 6287.
(155) Yusov, A. B.; Fedosseev, A. M.; Delegard, C. H. *Radiochim. Acta* **2004**, *92*, 869.
(156) Connick, R. E.; McVey, W. H. *J. Am. Chem. Soc.* **1949**, *71*, 1534.
(157) Ockenden, D. W.; Welch, G. A. *J. Chem. Soc* **1956**, *1*, 3358.
(158) (a) Costanzo, D. A.; Biggers, R. E.; Bell, J. T. *J. Inorg. Nucl. Chem.* **1973**, *35*, 609. (b) Toth, L. M.; Friedman, H. A.; Osborne, M. M. *J. Inorg. Nucl. Chem.* **1981**, *43*, 2929. (c) Kim, J. I. In *Handbook on the Physics and Chemistry of the Actinides*; Freeman, A. J., Keller, C., Eds.; Elsevier: Amsterdam, 1988.
(159) Cho, H. R.; Marquardt, C. M.; Neck, V.; Seibert, A.; Walther, C.; Yun, J. I.; Fanghänel, T. In *Recent Advances in Actinide Science*; May, I., Alvarez, R., Bryan, N., Eds.; Royal Society of Chemistry Publishing: Cambridge, UK, 2005.
(160) Denecke, M. A. *Coord. Chem. Rev.* **2006**, *205*, 730.
(161) Thiyagarajan, P.; Diamond, H.; Soderholm, L.; Horwitz, E. P.; Toth, L. M.; Felker, L. K. *Inorg. Chem.* **1990**, *29*, 1902.
(162) Kasha, M. In *The Transuranium Elements*; Seaborg, G. T., Katz, J. J., Manning, W. M., Eds.; McGraw-Hill Inc.: New York, 1949.
(163) Harvey, B. G.; Heal, H. G.; Maddock, A. G.; Rowley, E. L. *J. Chem. Soc.* **1947**, *1*, 1010.
(164) Kim, J. I.; Buckau, G.; Baumgärtner, F.; Moon, H. C.; Lux, D. In *Scientific Basis for Nuclear Waste Management*; McVay, G. L., Ed.; Elsevier: New York, 1984; Vol. *7*.
(165) (a) Choppin, G. R.; Bond, A. H.; Hromadka, P. M. *J. Radioanal. Nucl. Chem.* **1997**, *219*, 203. (b) Efurd, D. W.; Runde, W.; Banar, J. C.; Janecky, D. R.; Kaszuba, J. P.; Palmer, P. D.; Roensch, F. R.; Tait, C. D. *Environ. Sci. Technol.* **1998**, *32*, 3893.
(166) (a) Bell, J. T.; Costanzo, D. A.; Biggers, R. E. *J. Inorg. Nucl. Chem.* **1973**, *35*, 623. (b) Bell, J. T.; Coleman, C. F.; Costanzo, D. A.; Biggers, R. E. *J. Inorg. Nucl. Chem.* **1973**, *35*, 629. (c) Newton, T. W.; Hobart, D. E.; Palmer, P. D. *Radiochim. Acta* **1986**, *39*, 139.
(167) Lemire, R. J.; Fuger, J.; Nitsche, H.; Potter, P.; Rand, M. H.; Rydberg, J.; Spahiu, K.; Sullivan, J. C.; Ullman, W. J.; Vitorge, P.; Wanner, H. *Chemical Thermodynamics of Neptunium and Plutonium*; Elsevier, North-Holland: Amsterdam, 2001.
(168) He, S. L.; Oddo, J. E.; Tomson, M. B. *J. Colloid Interface Sci.* **1994**, *162*, 297.
(169) Fujiwara, K.; Yamana, H.; Fujii, T.; Moriyama, H. *J. Nucl. Fuel Cycle Environ.* **2001**, *7*, 17.
(170) (a) Perez-Bustamante, J. A. *Radiochim. Acta* **1965**, *4*, 67. (b) Rai, D.; Ryan, J. L. *Radiochim. Acta* **1982**, *30*, 213. (c) Rai, D. *Radiochim. Acta* **1984**, *35*, 97. (d) Kim, J. I.; Kanellakopulos, B. *Radiochim. Acta* **1989**, *48*, 145. (e) Fujiwara, K.; Yamana, H.; Fujii, T.; Moriyama, H. *Radiochim. Acta* **2002**, *90*, 857.
(171) Ankudinov, A. L.; Conradson, S. D.; de Leon, J. M.; Rehr, J. J. *Phys. Rev. B* **1998**, *57*, 7518.
(172) (a) Rai, D.; Swanson, J. L. *Nucl. Tech.* **1981**, *54*, 107. (b) Silva, R. J.; Nitsche, H. In *Advances in Plutonium Chemistry, 1967*−*2000*; Hoffman, D. C., Ed.; American Nuclear Society: La Grange park, IL, 2002. (c) Haschke, J. M.; Oversby, V. M. *J. Nucl. Mater.* **2002**, *305*, 187.
(173) Reed, D. T.; Lucchini, J. F.; Aase, S. B.; Kropf, A. J. *Radiochim. Acta* **2006**, *94*, 591.
(174) Olsson, M. *Radiochim. Acta* **2006**, *94*, 575.
(175) Triay, I. R.; Hobart, D. E.; Mitchell, A. J.; Newton, T. W.; Ott, M. A.; Palmer, P. D.; Rundberg, R. S.; Thompson, J. L. *Radiochim. Acta* **1991**, *52*−*3*, 127.
(176) Rundberg, R. S.; Mitchell, A. J.; Triay, I. R.; Torstenfelt, N. B. Materials Research Society Fall Meeting; Boston, MA, 1988; p 243.
(177) (a) Friedmann, H. A.; Toth, L. M.; Bell, J. T. *J. Inorg. Nucl. Chem.* **1977**, *39*, 123. (b) Haschke, J. M.; Haire, R. G. In *Advances in Plutonium Chemistry, 1967*−*2000*; Hoffman, D. C., Ed.; American Nuclear Society: La Grange park, IL, 2002.
(178) Johnson, G. L.; Toth, L. M. *Report* **1978**, *3*, 43386.
(179) (a) Conradson, S. D.; Begg, B. D.; Clark, D. L.; den Auwer, C.; Ding, M.; Dorhout, P. K.; Espinosa-Faller, F. J.; Gordon, P. L.; Haire, R. G.; Hess, N. J.; Hess, R. F.; Keogh, D. W.; Lander, G. H.; Manara, D.; Morales, L. A.; Neu, M. P.; Paviet-Hartmann, P.; Rebizant, J.; Rondinella, V. V.; Runde, W.; Tait, C. D.; Veirs, D. K.; Villella, P. M.; Wastin, F. *J. Solid State Chem.* **2005**, *178*, 521. (b) Conradson, S. D.; Abney, K. D.; Begg, B. D.; Brady, E. D.; Clark, D. L.; den Auwer, C.; Ding, M.; Dorhout, P. K.; Espinosa-Faller, F. J.; Gordon, P. L.; Haire, R. G.; Hess, N. J.; Hess, R. F.; Keogh, D. W.; Lander, G. H.; Lupinetti, A. J.; Morales, L. A.; Neu, M. P.; Palmer, P. D.; Paviet-Hartmann, P.; Reilly, S. D.; Runde, W. H.; Tait, C. D.; Veirs, D. K.; Wastin, F. *Inorg. Chem.* **2004**, *43*, 116.
(180) (a) Romanovski, V. V.; Palmer, C. E.; Shaw, H. F.; BOurcier, W. L.; Jardine, L. J. *Plutonium Futures*; Santa Fe, NM, 2000; p 1. (b) Nitsche, H.; Roberts, K.; Xi, R. H.; Prussin, T.; Becraft, K.; Almahamid, I.; Silber, H. B.; Carpenter, S. A.; Gatti, R. C.; Novak, C. F. *Radiochim. Acta* **1994**, *66*−*67*, 3.
(181) Walther, C.; Rothe, J.; Fuss, M.; Büchner, S. *Actinide Res. Q.* **2009**, *17*, 19.
(182) Haschke, J. M.; Allen, T. H.; Morales, L. A. *Science* **2000**, *287*, 285.
(183) Haschke, J. M. *J. Nucl. Mater.* **2007**, *362*, 60.
(184) (a) Artyukhin, P. I.; Medvedovskii, V. I.; Gelman, A. D. *Russ. J. Inorg. Chem.* **1959**, *4*, 596. (b) Rabideau, S. W.; Lemons, J. F. *J. Am. Chem. Soc.* **1951**, *73*, 2895.
(185) (a) Conradson, S. D.; Begg, B. D.; Clark, D. L.; Den Auwer, C.; Espinosa-Faller, F. J.; Gordon, P. L.; Hess, N. J.; Hess, R.; Keogh, D. W.; Morales, L. A.; Neu, M. P.; Runde, W.; Tait, C. D.; Veirs, D. K.; Villella, P. M. *Inorg. Chem.* **2003**, *42*, 3715. (b) Haschke, J. A. *J. Nucl. Mater.* **2004**, *334*, 225. (c) Haschke, J. M. *J. Nucl. Mater.* **2005**, *344*, 8. (d) Korzhavyi, P. A.; Vitos, L.; Andersson, D. A.; Johansson, B. *Nat. Mater.* **2004**, *3*, 225.
(186) Wang, Q.; Li, G.-D.; Xu, S.; Li, J.-X.; Chen, J.-S. *J. Mater. Chem.* **2008**, *18*, 1146.

(187) Wu, H.; Yang, Y.; Cao, Y. C. *J. Am. Chem. Soc.* **2006**, *128*, 16522.
(188) Zhang, Z. T.; Konduru, M.; Dai, S.; Overbury, S. H. *Chem. Commun.* **2002**, 2406.
(189) Nenoff, T. M.; Jacobs, B. W.; Robinson, D. B.; Provencio, P. P.; Huang, J.; Ferreira, S.; Hanson, D. J. *Chem. Mater.* **2011**, *23*, 5185.
(190) Takeuchi, K.; Kuga, Y.; Satooka, S.; Okuyama, K. *J. Aerosol Sci.* **1998**, *29*, 1027.
(191) Gil, D.; Malmbeck, R.; Spino, J.; FanghÃ¤nel, T.; Dinnebier, R. E. *Radiochim. Acta* **2010**, *98*, 77.
(192) Rousseau, G.; Fattahi, M.; Grambow, B.; Desgranges, L.; Boucher, F.; Ouvrard, G.; Millot, N.; NiÄpce, J. C. *J. Solid State Chem.* **2009**, *182*, 2591.
(193) Burns, P. C. *C. R. Chim.* **2010**, *13*, 737.
(194) Vlaisavljevich, B.; Gagliardi, L.; Burns, P. C. *J. Am. Chem. Soc.* **2010**, *132*, 14503.
(195) Schimmelpfennig, B. In *Actinide Nanoparticle Research*; Kalmykow, S., Denecke, M. A., Eds.; Springer: Berlin Heidelberg, 2011.
(196) Burns, P. C.; Kubatko, K.-A.; Sigmon, G.; Fryer, B. J.; Gagnon, J. E.; Antonio, M. R.; Soderholm, L. *Angew. Chem., Int. Ed.* **2005**, *44*, 2135.
(197) Forbes, T. Z.; McAlpin, J. G.; Murphy, R.; Burns, P. C. *Angew. Chem., Int. Ed.* **2008**, *47*, 2824.
(198) Sigmon, G. E.; Ling, J.; Unruh, D. K.; Moore-Shay, L.; Ward, M.; Weaver, B.; Burns, P. C. *J. Am. Chem. Soc.* **2009**, *131*, 16648.
(199) Ling, J.; Qiu, J.; Burns, P. C. *Inorg. Chem.* **2012**, *51*, 2403.
(200) Unruh, D. K.; Ling, J.; Qiu, J.; Pressprich, L.; Baranay, M.; Ward, M.; Burns, P. C. *Inorg. Chem.* **2011**, *50*, 5509.
(201) Takao, S.; Takao, K.; Kraus, W.; Ernmerling, F.; Scheinost, A. C.; Bernhard, G.; Hennig, C. *Eur. J. Inorg. Chem.* **2009**, 4771.
(202) Krivovichev, S. V. *Eur. J. Inorg. Chem.* **2010**, 2594.
(203) (a) Krivovichev, S. V.; Kahlenberg, V.; Kaindl, R.; Mersdorf, E.; Tananaev, I. G.; Myasoedov, B. F. *Angew. Chem., Int. Ed.* **2005**, *44*, 1134. (b) Krivovichev, S. V.; Kahlenberg, V.; Tananaev, I. G.; Kaindil, R.; Mersdorf, E.; Myasoedov, B. F. *J. Am. Chem. Soc.* **2005**, *127*, 1072.
(204) Diwu, J.; Wang, S.; Albrecht-Schmitt, T. E. *Inorg. Chem.* **2012**, *51*, 4088.
(205) Diwu, J.; Good, J. J.; DiStefano, V. H.; Albrecht-Schmitt, T. E. *Eur. J. Inorg. Chem.* **2011**, 1374.
(206) Wu, H.; Chen, O.; Zhuang, J.; Lynch, J.; LaMontagne, D.; Nagaoka, Y.; Cao, Y. C. *J. Am. Chem. Soc.* **2011**, *133*, 14327.
(207) IAEA. "Co-ordinated research programme on radioactive particle", International Atomic Energy Agency CRP G41003, 2001.
(208) ICRP. "1990 Recommendations ICRP Publication 60", 1991.
(209) Hardman, R. *Environ. Health Perspect.* **2006**, *114*, 165.
(210) Brown, G. E. J.; Calas, G. *Geochemical Perspectives*, 2012; Vol. *1*, pp 611−627.
(211) Moore, K. T.; Marianetti, C. A.; Lander, G. H. *MRS Bull.* **2010**, *35*, 841.
(212) Hudry, D.; Apostolidis, C.; Walter, O.; Gouder, T.; Courtois, E.; Kübel, C.; Meyer, D. *Chem.-Eur. J.* **2012**, *18*, 8283.
(213) Kretschmar, R.; Schäfer, T. *Elements* **2005**, *1*, 205.